5-2012

GLOTTAL EXCITATION EXTRACTION OF VOICED SPEECH - JOINTLY PARAMETRIC AND NONPARAMETRIC APPROACHES

Yiqiao Chen
Clemson University, rls_lms@yahoo.com

GLOTTAL EXCITATION EXTRACTION OF VOICED SPEECH－ JOINTLY PARAMETRIC AND NONPARAMETRIC APPROACHES

A Dissertation
Presented to
the Graduate School of
Clemson University

In Partial Fulfillment
of the Requirements for the Degree
Doctor of Philosophy
Electrical Engineering

---

by
Yiqiao Chen
May, 2012

Accepted by:
John N. Gowdy, Committee Chair
Robert J. Schalkoff
Stanley T. Birchfield
Elena Dimitrova

ABSTRACT

The goal of this dissertation is to develop methods to recover glottal flow pulses, which contain biometrical information about the speaker. The excitation information estimated from an observed speech utterance is modeled as the source of an inverse problem.

Windowed linear prediction analysis and inverse filtering are first used to deconvolve the speech signal to obtain a rough estimate of glottal flow pulses. Linear prediction and its inverse filtering can largely eliminate the vocal-tract response which is usually modeled as infinite impulse response filter. Some remaining vocal-tract components that reside in the estimate after inverse filtering are next removed by maximum-phase and minimum-phase decomposition which is implemented by applying the complex cepstrum to the initial estimate of the glottal pulses. The additive and residual errors from inverse filtering can be suppressed by higher-order statistics which is the method used to calculate cepstrum representations.

Some features directly provided by the glottal source's cepstrum representation as well as fitting parameters for estimated pulses are used to form feature patterns that were applied to a minimum-distance classifier to realize a speaker identification system with very limited subjects.

ACKNOWLEDGMENTS

I would like to appreciate the long-term support over the years provided by Dr. John N. Gowdy, my advisor, since the first time I met him. This dissertation cannot be completed without his guidance and patience.

Meanwhile, I wish to express my appreciation to Dr. Robert Schalkoff, Dr. Stanley Birchfield and Dr. Elena Dimitrova for their valuable comments and helpful suggestions in terms of this dissertation.

TABLE OF CONTENTS

Page

TITLE PAGE i

ABSTRACT ii

ACKNOWLEDGMENTS iii

LIST OF TABLES vi

LIST OF FIGURES vii

CHAPTER

I. INTRODUCTION AND OVERVIEW 1

Overview of Extraction of Glottal Flow Pulses 1
Structure of the dissertation 2

II. PHONETICS 4

The Physical Mechanism of Speech Production 4
Classifications of Speech Sounds 7

III. MODELS 11

Glottal Flow Pulse Modeling 11
Discrete-Time Modeling of Vocal Tract and Lips Radiation 19
Source-Filter Model for Speech Production 24

IV. THE ESTIMATION OF GLOTTAL SOURCE 27

Two Methods of Linear Prediction 27
Homomorphic Filtering 32
Glottal Closure Instants Detection 33
Parametric Approaches to Estimate Glottal Flow Pulses 35
Nonparametric Approaches to Estimate Glottal Flow Pulses 37

Summary 39

V. JOINTLY PARAMETRIC AND NONPARMETRIC ESTIMATION APPROACHES OF GLOTTAL FLOW PULSES I 40

Introduction 40
Odd-Order Linear Prediction Preprocessing and Inverse Filtering 44
Phase Decomposition 47
Waveform Simulations 49
Simulations of Data Fitting 52
Summary 64

VI. JOINTLY PARAMETRIC AND NONPARMETRIC ESTIMATION APPROACHES OF GLOTTAL FLOW PULSES II 66

Brief backgrounds on High-Order Statistics 67
Odd-Order Linear Prediction 69
Higher-Order Homomorphic Filtering 72
Simulation Results 77
Summary 81

VII. A SMALL SCALE SPEAKER IDENTIFIER WITH LIMITED EXCITING INFORMATION 83

Overall Scheme of the Speaker Identifier 84
Selection of Distinct Feature Patterns for Identifier 86

VIII. CONCLUSIONS 93

Jointly Parametric and Nonparametric Excitation Estimation For Real and Synthetic Speech 93
Features from Estimated Glottal Pulses for Speaker Identifier 95
Suggested Directions of Research 96

APPENDICES 98

A: Third-Order Cumulant and Bicepstrum of Output from a Linear System Excited by White Processes 99

REFERENCES 102

LIST OF TABLES

Table		Page
2.1	Phonetic category of American English	9
5.1	Comparison of parameters of synthetic and fitting excitation pulses from different methods	63
6.1	Comparison of parameters of synthetic and fitted excitation pulses	81
7.1	Speaker identification results for two different features	91

LIST OF FIGURES

Figure Page

2.1 Illustration of human speech production 5

2.2 The short-time frequency representation of a female speech utterance: "What is the mid-way?" 6

3.1 Normalized Rosenberg glottal model 12

3.2 Lijencrants-Fant model with shape-control parameters 14

3.3 LF models set by 3 different R_d values and their corresponding frequency responses 16

3.4 Time and frequency response of Rosenburg and LF model 17

3.5 Acoustic tube model of vocal tract 20

3.6 Illustration of -3 dB bandwidth between two dot lines for a resonance frequency at 2,000 Hz 22

3.7 Resonance frequencies of a speaker's vocal tract 23

3.8 The discrete-time model of speech production 26

5.1 Illustration of vocal-tract response from linear prediction analysis with overlapped Blackman windows 43

5.2 Analysis region after LP analysis 46

5.3 Finite-length complex cepstrum of $\tilde{\boldsymbol{e}}[n]$ 48

5.4 The odd-order LP and CC flow 49

5.5 Estimation of glottal pulse for a real vowel /a/ 50

5.6 Comparison between (a) Original pulse and (b) Estimated pulse 51

5.7 (a) Synthetic LF excitation pulse (b) Estimated pulse (black dash line) by LP+CC method 60

List of Figures (Continued)

Figure Page

5.8 Estimated pulse (black dash line) by IAIF method 62

5.9 Estimated pulse (black dash line) by ZZT method 62

6.1 Illustration of bispectrum of $\sin\frac{\pi}{2}n + \sin\frac{\pi}{9}n$ 69

6.2 Analysis region after LP analysis 72

6.3 The 3rd-order cumulant of the finite-length sequence $\mathbf{y}_m$ 73

6.4 Normalized GFP estimation of a real vowel /a/ 77

6.5 Illustration of (a) Original GFP used to generate voiced Speech sequence (b) Estimated GFP resulting from LP and bicepstrum-decomposition .. 78

6.6 Workflow to recover exciting synthetic glottal pulse 79

6.7 (a) Synthetic LF excitation pulse (b) Estimated pulse (black dash line) and fitted pulse (gray solid line) 80

7.1 Speaker identification system to choose models 85

7.2 Decision boundaries for centroids based on Minimum Euclidean Distance 85

7.3 Illustrations of a single estimated glottal flow derivatives and their fitting pulses 87

. 7.4 Illustrations of complex cepstrum coefficients of a single estimated glottal flow pulse and extraction of low cepstrum-frequency quantities 90

CHAPTER ONE

INTRODUCTION AND OVERVIEW

The topic of the dissertation, the extraction of glottal flow pulses for vowels, has a potential benefit for a wide range of speech processing applications. Though some progress has been made in extracting glottal source information and applying this data to speech synthesis and recognition, there is still room for enhancement of this process. This chapter gives a brief overview of research on this topic, and the motivation for extraction of glottal flow pulses. The structure of the dissertation is also presented.

Overview of Extraction of Glottal Flow Pulses

The extraction of glottal flow pulses can provide important information for many applications in the field of speech processing since it can provide information that is specific to the speaker. This information is useful for speech synthesis, voiceprint processing, and speaker recognition. Three major components: glottal source, vocal tract and lips radiation, form human speech sounds based on Fant's acoustic discoveries [1]. If we can find a way to estimate the glottal source, the vocal-tract characteristics can be estimated by extracting the glottal source from the observed speech utterance. As voiced sounds are produced, the nasal cavity coupling with oral cavity is normally not a major factor. Therefore, speech researchers focused on properties and effects of vocal-tract response. The high percentage of voiced sounds, especially vowels, has been another motivation for research of this domain.

Given observed speech signals as input data, we can formulate a task to extract the glottal source as an inverse problem. There is no way to know what actual pulses are like for any voiced sounds. It makes the problem much harder than those ones in communication channels for which information source is known. Some glottal pulse extraction methods [2], [3] have been proposed as a result of acoustic experiments and statistical analysis. They might not be very accurate but they at least can provide rough shapes for pulses. The earliest result came from establishing an electrical network for glottal waveform analog inverse filtering [2]. Thereafter, some better improvements have been made in the past two decades to recover these pulses using signal processing methods that involve recursive algorithms for linear prediction analysis. However, existing methods here not been able to attain both high accuracy and low complexity. The time-variance of these excitation pulses and vocal tract expands the difficulty of the extraction problem. The lack of genuine pulses makes it challenging for researchers to evaluate their results accurately. In past papers [4], [5] researchers adapted the direct shape comparison between an estimated pulse from a synthesized speech utterance and the original synthetic excitation pulse. As part of our evaluation, we will parameterize our estimated pulses and use these as inputs of a small scale speaker identification system.

Structure of the dissertation

The next two chapters present backgrounds for basic phonetics, glottal models and the source-filter model as well as its discrete-time representations. After a background discussion, we will introduce the theme of the dissertation on how to extract

glottal flow pulses. Mainstream glottal flow pulses estimation methods are discussed in Chapter 4. Two jointly parametric and nonparametric methods are extensively discussed in Chapter 5 and 6. The parameterization of estimated glottal flow pulses and their results from a vector quantization speaker identification system with limited subjects will be discussed in Chapter 7. Then a summary section concludes the dissertation.

CHAPTER TWO

PHONETICS

In this chapter, we will discuss the production of speech sounds from viewpoints of acoustics and linguistics.

The Physical Mechanism of Speech Production

The generation of human speech can be illustrated by the system shown in Figure 2.1. The diaphragm is forced by abdominal muscles to push air out of the lungs through trachea into the glottis, a slit-like orifice between the two folds, movements of which affect air flow. As the speech is produced, it is adjusted by the varying shape of the vocal tract above larynx. The air flow forms speech when it leaves the lips and nose. The pharynx connects the larynx with the oral cavity that is the main cavity of the vocal tract. It can be altered because of activities of the palate, the tongue, the teeth and the lips.

There are two key factors that researchers cannot ignore as they study the above acoustic process of speech production: vocal tract and glottal source. The vocal tract where resonances occur in the speech production process can be represented as a multi-tube lossless model from the vocal folds to the lips with an auxiliary path, the nasal cavity. The locations of resonances are controlled by the physical shape of the vocal tract of the speaker. Likewise, the shape of vocal tract can be characterized by these resonance frequencies. This has been the theoretical basis for many speech synthesis and speaker recognition applications. These resonance frequencies were called formants by speech pioneers because they can form overall spectrum of the speech utterance.

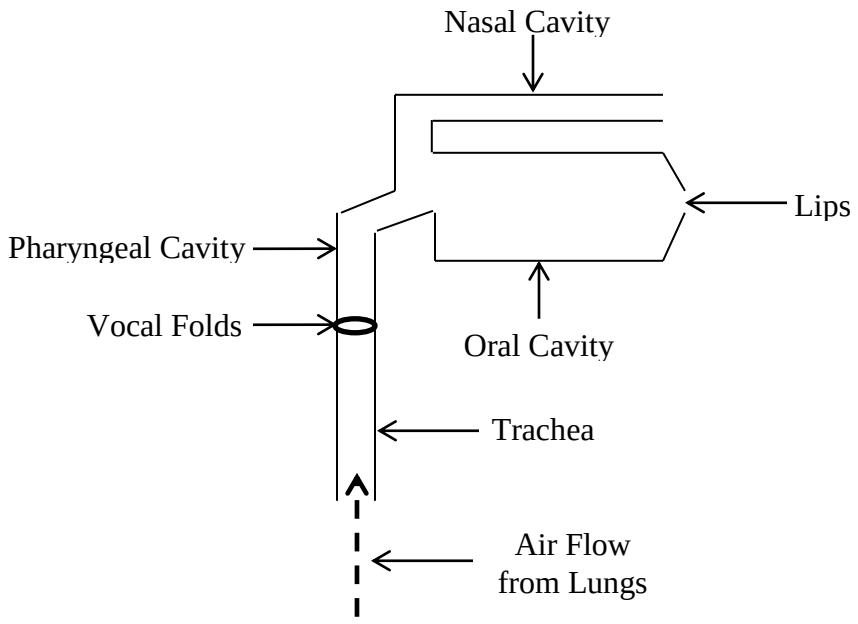

Figure 2.1 Illustration of human speech production

The formants, shown the spectrogram in the Figure 2.2, ordered from lowest frequency to highest frequency, are symbolized by F_1, F_2, F_3,…. They are represented by horizontal darker strips, and they vary with time. This phenomenon indicates that our vocal tract has dynamic characteristics. The lower-frequency formants dominate the speaker's vocal-tract response from an energy perspective.

In above process, air flow from vocal folds results in a rhythmic open and closed

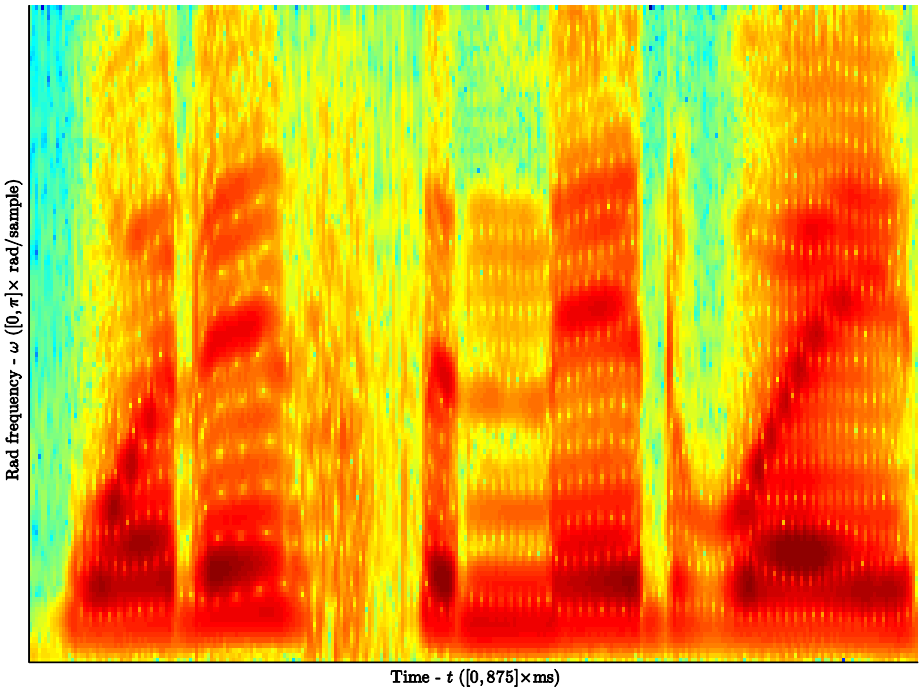

Figure 2.2 The short-time frequency representation of a female speech utterance: "What is the mid-way?"

phase of glottal source. In the frequency domain, the glottal flow pulses are normally characterized as a low-pass filtering response [6]. On the other hand, the time interval between two adjacent vocal-folds opens is called pitch or fundamental period, the reciprocal of which is called fundamental frequency. The period of glottal source is an important physical feature of a speaker along with the vocal tract determining formants.

The glottal source in fact plays a role of excitation to both the oral and nasal cavities. Speech has two elementary types: voiced and unvoiced, or a combination of them [7], e.g., plosives, and voiced fricatives.

Voiced excitations are produced from a sort of quasi-periodic movement of vocal-folds while air flow is forced through glottis. Consequently, a train of quasi-periodic puffs of air occurs. The unvoiced excitation is a disordering turbulence caused by air flow passing a narrow constriction at some point inside the vocal tract. In most cases, it can be treated as noise. These two excitation types and their combinations can be utilized by continuous or discrete-time models.

Classifications of Speech Sounds

In linguistics, a phoneme is the smallest unit of speech distinguishing one word (or word element) from another. And phones triggered by glottal excitations refer to actual sounds in a phoneme class.

We briefly list some categories of phonemes and their corresponding acoustic features [7]:

Fricatives: Fricatives are produced by exciting the vocal tract with a stable air flow which becomes turbulent at some point of constriction along the oral tract. There are voiced fricatives in which vocal folds vibrate simultaneously with noise generation, e.g., /v/. But vocal folds in terms of unvoiced fricatives are not vibrating, e.g., /h/.

Plosives: Plosives are almost instantaneous sounds that are produced by suddenly releasing the pressure built up behind a total constriction in the vocal tract. Vocal folds in terms of voiced plosives vibrate, e.g., /g/. But there are no vibrations for unvoiced plosives, e.g., /k/.

Affricates: Affricates are formed by rapid transitions from the oral shape pronouncing a plosive to that pronouncing a fricative. There can be voiced, e.g., /J/, or unvoiced, e.g., /C/.

Nasals: These are produced when there is voiced excitation and the lips are closed, so that the sound emanates from the nose.

Vowels: These are produced by using quasi-periodic streams of air flows though vocal folds to excite a speaker's vocal-tract in constant shape, e.g., /u/. Different vowels have different vocal-tract configurations of the tongue, the jaw, the velum and the lips of the speaker. Each of the vowels is distinct from others due to their specific vocal-tract's shape that results in distinct resonance, locations and bandwidths.

Diphthongs: These are produced by rapid transition from the position to pronounce one vowel to another, e.g., /W/.

The list of phonemes used in American English language is summarized in Table 2.1.

The study of vowels has been an important topic for almost any speech applications ranging from speech and speaker recognition to language processing. There are a number of reasons that make vowels so important.

The frequency of occurring of vowels leads them to be the major group of subjects in the field of speech analysis. As vowels are present in any word in the English language, researchers can find very rich information for all speech processing applications. And they can be distinguished by locations, widths and magnitudes of formants. These parameters are determined by the shape of a speaker's oral cavity.

Finally, the glottal puffs as excitations to vowels are speaker-specific and quasi-periodic. Intuitively, the characteristics of these pulses as glottal excitations can be considered as a type of features [8] - [11] used for speaker recognition and other applications.

Continuant	Vowels	Front	/i/,/I/,/e/,/E/,/@/	
		Mid	/R/,/x/,/A/	
		Back	/u/,U/,/o/,/c/,/a/	
	Consonants	Fricatives	Voiced	/v/,/D/,/z/,/Z/
			Unvoiced	/f/,/T/,/s/,/S/
		Whisper	/h/	
		Affricates	/J/,/C/	
		Nasals	/m/,/n/,/G/	
Noncontinuant	Diphthongs	/Y/,/W/,/O/,/yu/		
	Semivowels	Liquids	/r/,/l/	
		Glides	/w/,/y/	
	Consonants	Voiced	/b/,/d/,/g/	
		Unvoiced	/p/,/t/,/k/	

Table 2.1 Phonetic category of American English

However, not until some physical characteristics of speech waves were calibrated by experiments that researchers started to assume some important properties of these excitation signals [2]. These characteristics laid a milestone to investigate the excitation,

channel and lips radiation quantitatively in terms of human speech. Excitation, or glottal sources, will be the subject through the dissertation. Some existing models of glottal source will be extensively discussed in next chapter.

CHAPTER THREE

MODELS

The study of speech production has existed for several decades ago. However, little progresses in analyzing the excitation of speech sounds had been made until some researchers purposed methods modeling glottal flow pulses [6] - [10]. By combining the glottal flow pulses models, glottal noise models and vocal tract resonance frequencies transmission models, we can build an overall discrete-time speech production system. Furthermore, the synthesis of a whole utterance of speech depends on the analysis of interactions between glottal sources and vocal tract of speakers by using digital processing techniques.

Glottal Flow Pulse Modeling

For voiced phonemes, typically vowels, researchers have endeavored to recover the glottal flows to characterize and represent distinct speakers in speech synthesis and speaker recognition. The term, glottal flow, is an acoustic expression of air flow that interacts with vocal tract. Consequently, it is helpful to find some parameters to describe models and regard these parameters as some features of speakers. The periodic characteristic of the flow is determined by the periodic variation of glottis: Each period includes an open phase, return phase and close phase. The time-domain waveform representing volume velocity of glottal flows as excitations coming from glottis has been an object for modeling in the past decades.

Rosenberg, Liljencrants and Fant were among those most successful pioneers who

contributed to find non-interactive glottal pulse models.

Rosenberg proposed several models [6] to represent an ideal glottal pulse. The preferred model is referred as Rosenberg-B, which represents the glottal pulse as

$$g(t) = \begin{cases} 3\left(\frac{t}{T_p}\right)^2 - 2\left(\frac{t}{T_p}\right)^3, & 0 \le t < T_p \\ 1 - \left(\frac{t - T_p}{T_n}\right)^2, & T_p \le t < T_p + T_n \end{cases} \tag{3.1}$$

This is the first model to relate the quasi-periodic glottal excitations shown in Figure 3.1 to the periodic activities of vocal folds. Vocal folds are assumed to have a sudden closure in their return phase, as shown in the Figure 3.1.

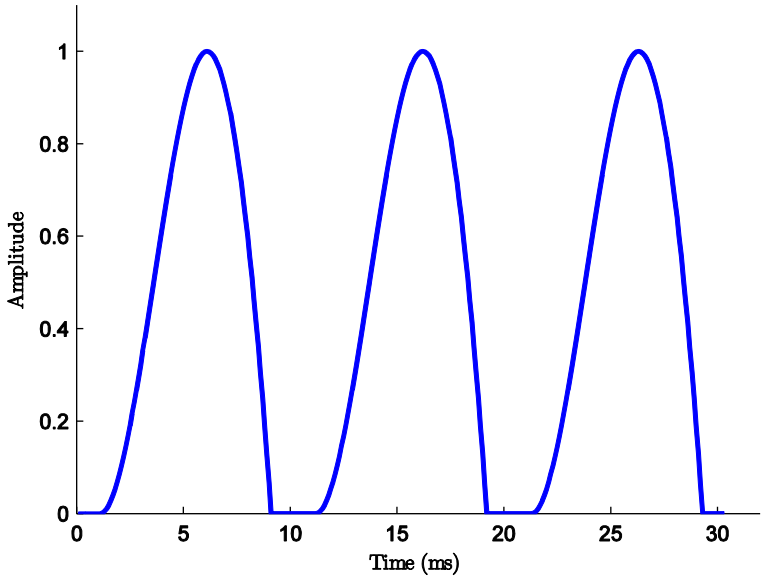

Figure 3.1 Normalized Rosenberg glottal model

Klatt and Klatt [9] introduced different parameters to control the Rosenberg glottal model.

A derivative model of glottal flow pulse [10], was proposed in 1986 by Fant. The Liljencrants-Fant (LF) model contains the parameters clearly showing the glottal open, closed and return phases, and the speeds of glottal opening and closing. It allows for an incomplete closure or for a return phase of growing closure rather than a sudden closure, a discontinuity in glottal model output.

Let $g(t)$ be a single pulse. We might assume

$$\int_0^{T_c} g'(t)\, dt = 0 \tag{3.2}$$

then the net gain of the $g'(t)$ within both close and open phase is zero.

The derivative of $g(t)$ can be modeled by [11]

$$g'(t) = \begin{cases} E_0 e^{\alpha(t-T_o)} \sin[\omega_o(t-T_o)], & T_o \le t < T_e \\ E_1\left[e^{-\beta(t-T_e)} - e^{-\beta(T_c-T_e)}\right], & T_e \le t < T_c \\ 0, & 0 \le t < T_o \end{cases} \tag{3.3}$$

where E_0 and E_1 are defined in terms of a parameter E_e by

$$E_1 = \frac{E_e}{1 - exp[-\beta(T_c - T_e)]}$$

and

$$E_0 = \frac{E_e}{exp[\alpha(T_e - T_o)]\, sin[\omega_o(T_e - T_o)]}.$$

Thus, the glottal model can be expressed by 7 parameters [11]: T_o, the starting time of opening phase; T_e, the starting time of return phase[1]; T_c, the starting time of

[1] The starting time of return phase is not defined as the peak value of a complete glottal pulse.

closed phase; Ω_o, frequency of a sinusoidal signal modulated by exponentially decreasing signal in open phase; E_e, the flow derivative at T_e; α, the ratio of E_e to the largest positive value of $g'(t)$; β, an exponential factor that control the convergence rate of the model from T_e to zero (see Figure 3.2) where α, E_0 and Ω_o control the shape of open phase and E_1 and β control the shape of the return phase.

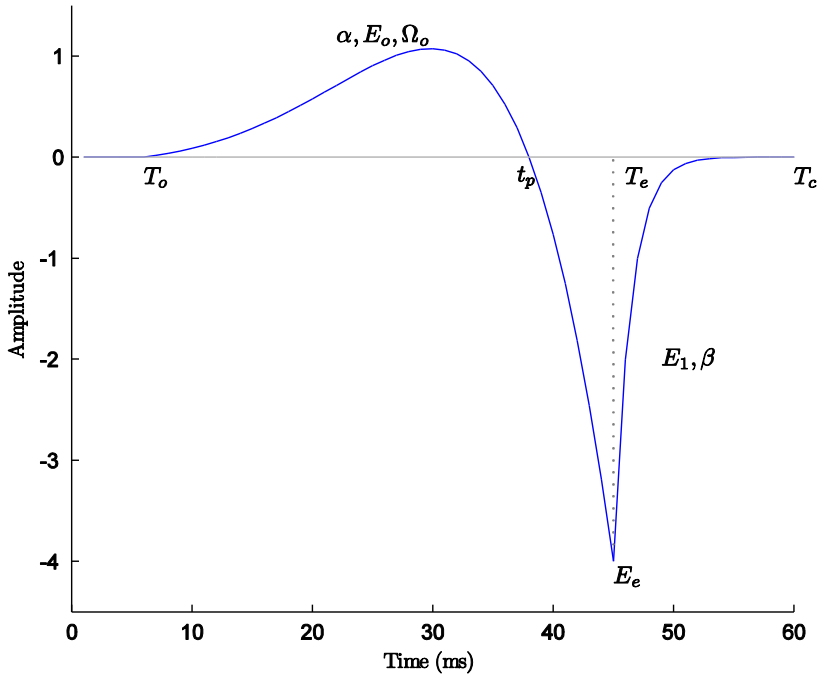

Figure 3.2 Lijencrants-Fant model with shape-control parameters

The transformed LF model as an extension of the original LF model was proposed in 1995 [12]. It uses a new set of R parameters to represent the T parameters T_o, T_e and T_a

involved in the LF model (effective duration of the return phase) and T_p (the time of zero glottal derivative). And a basic shape parameter R_d is

$$R_d \cong (0.5 + 1.2R_k)\left(\frac{R_k}{4R_g} + R_a\right)/0.11 \tag{3.4}$$

where R_a, R_a and R_g are obtained as

$$\begin{cases} R_a = \dfrac{T_a}{T_o} \\ R_k = \dfrac{T_e - T_p}{T_p} \\ R_g = \dfrac{T_o}{2T_p} \end{cases} . \tag{3.5}$$

Figure 3.3 shows a variety of LF models corresponding to different R_d values. The use of the R_d parameter largely simplifies the means to control the LF model. If there is a need for fitting a glottal flow pulse $\mathrm{g}(t)$ by an LF mode $\hat{\mathrm{g}}(t)$, then a least-squares optimization problem exists with the objective function and its constraints which can be represented as

$$\begin{aligned} &\arg\min_{R_d,T_o,T_e,T_c} \|\mathbf{g} - \hat{\mathbf{g}}\| \\ \text{subject to} \quad &0.3 \le R_d \le 2.7 \\ &0 < T_o < T_e < T_c \, . \end{aligned} \tag{3.6}$$

Both the Rosenberg and Liljencrants-Fant models had been proved to have spectral tilt in their frequency representations. The location of the peak of the spectral tilt is right at the origin for a Rosenberg model and close to the origin for LF model shown in Figure 3.4.

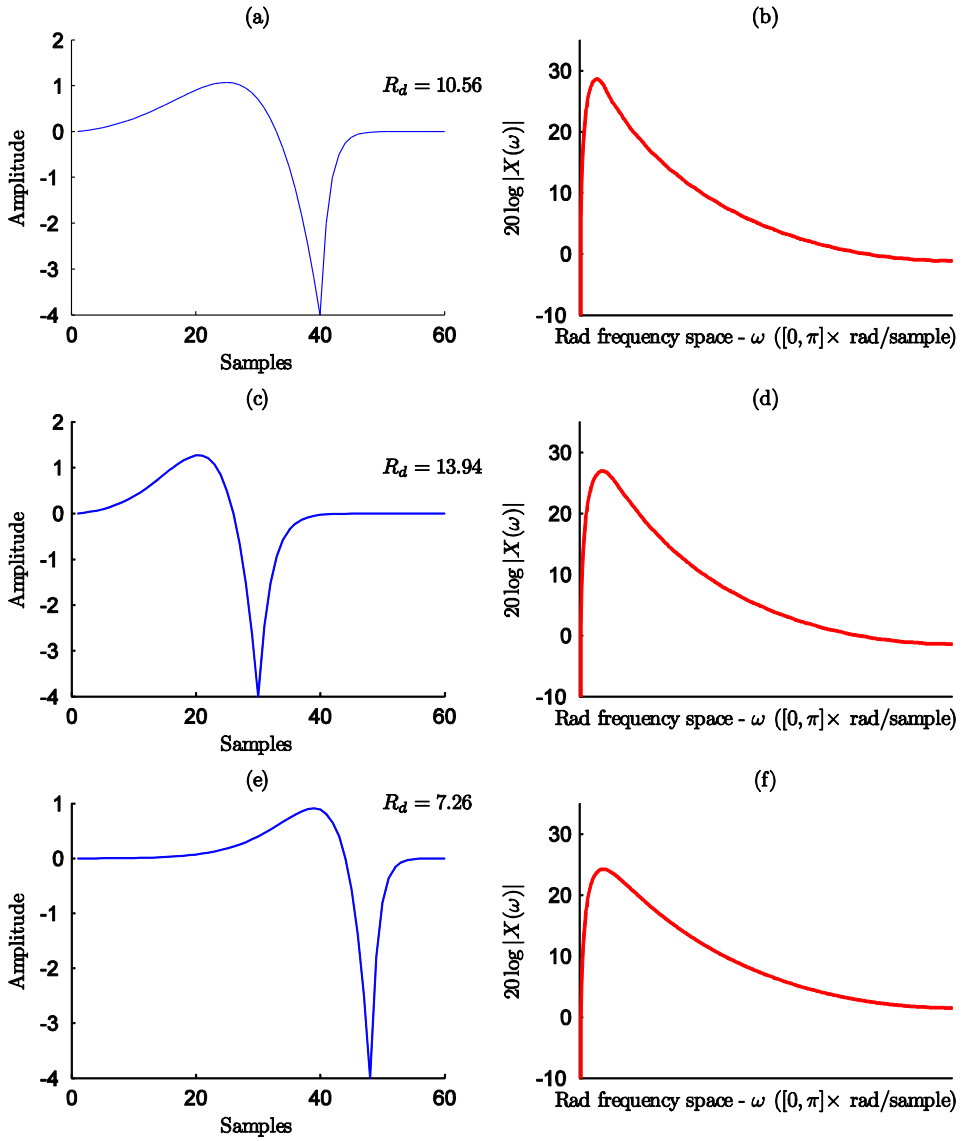

Figure 3.3 LF models set by 3 different Rd values and their corresponding frequency responses

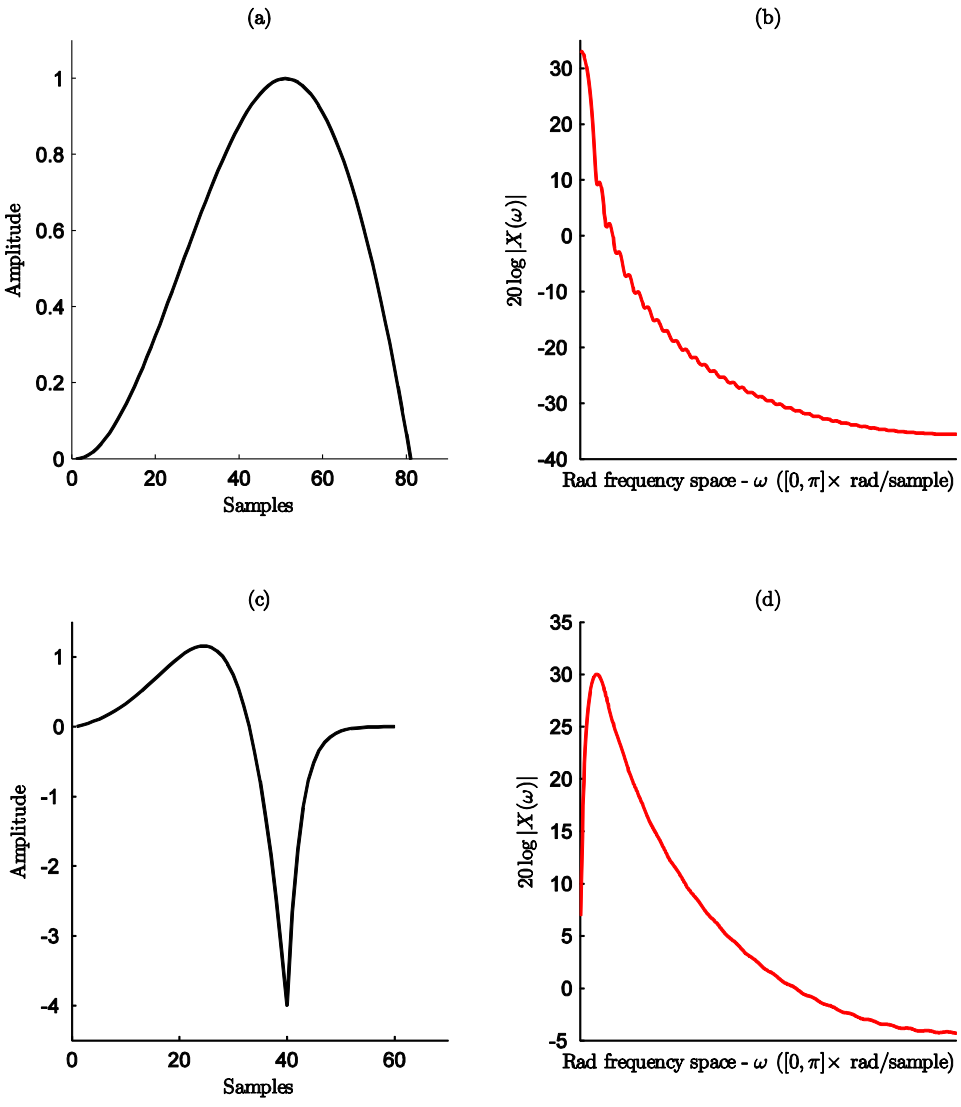

Figure 3.4 Time and frequency response of Rosenburg and LF model (a) Rosenburg model (b) Frequency response of (a) (c) LF model (d) Frequency response of (c)

Consequently, low-pass filtering effects in terms of the magnitude of frequency response can be approximations to these glottal models.

After they reviewed the glottal source in the time domain and frequency domain, Henrich, Doval and d'Alessandro proposed another Causal-Anticausal Linear Model (CALM) [13] which considers the glottal source the impulse response of a linear filter. They also quantitatively analyzed the spectral tilt with different model parameters. Expressions of Rosenberg and Klatt as well as LF models were investigated in both magnitude frequency and phase frequency domain. They proposed that the LF glottal model itself can be regarded as a result of the convolution of two truncated signals, one causal and one anti-causal, based on its analytical form. The open phase is contributed by a causal signal; on the other hand, the return phase is contributed by an anti-causal signal. Glottal flow pulse modeled by the LF model consists of minimum-phase and maximum-phase components, so it is mixed-phase. In this case, the finite-length anti-casual signal can be represented by zeros [13] which result in a simple polynomial rather than a ratio of polynomials which includes poles. The existence of the discontinuity at the tail of the return phase becomes a criterion for extracting the phase characteristic of glottal models. Thus, the Rosenburg model is maximum-phase, but the LF model is mixed-phase.

Aspiration, which is the turbulence caused by the vibration in terms of vocal-folds' tense closure, is considered to introduce random glottal noise to the glottal pulse. This may occur in a normal speech with phoneme /h/, but it seldom occurs in vowels.

Discrete-Time Modeling of Vocal Tract and Lips Radiation

As the major cavity involving in the production of voiced phonemes, the oral tract has a variety of cross-sections caused by altering the tongue, teeth, lips and jaw; its lengths varies from person to person. Fant [1] firstly modeled the vocal tract as a frequency-selective transmission channel.

The simplest speech model consists of a single uniform lossless tube with one end open end. The resonance frequencies of this model were called formants. The i th resonance frequency F_i can be calculated by

$$F_i = \frac{(2i-1)c}{4\ell}$$

where c is the transmission rate of the sound wave and ℓ is the length of the vocal tract as a single tube. Therefore, the length of the vocal tract will determine the resonance frequencies. The vocal tract was found to play a role as filter from acoustic analysis. Some acoustics pioneers [1], [14], [15] made great contributions to investigate the transfer function for vocal tract. This study involves a more complex but realistic model represented by multiple concatenated lossless tubes having different cross-sectional area, which is the extension of the single lossless tube model.

The vocal tract considered as the concatenation of tubes with different lengths and different cross-section area A_1, A_2, A_3 and A_4 is shown in Figure 2.4. The cross-section areas of tubes will determine the transmission coefficient $0 \leq \rho_i^+ \leq 1$ and reflection coefficient $0 \leq \rho_i^- \leq 1$ between adjacent tubes. (The concatenated vocal tract with transmission and reflection coefficients ρ_i^+, ρ_i^- can be modeled by a lattice-ladder

discrete-time filter). The transfer function $H(j\Omega)$ of vocal tract together with glottis and lips can be represented by these coefficients ρ_i^+, ρ_i^- from impedance, two-port and T-network analysis [16].

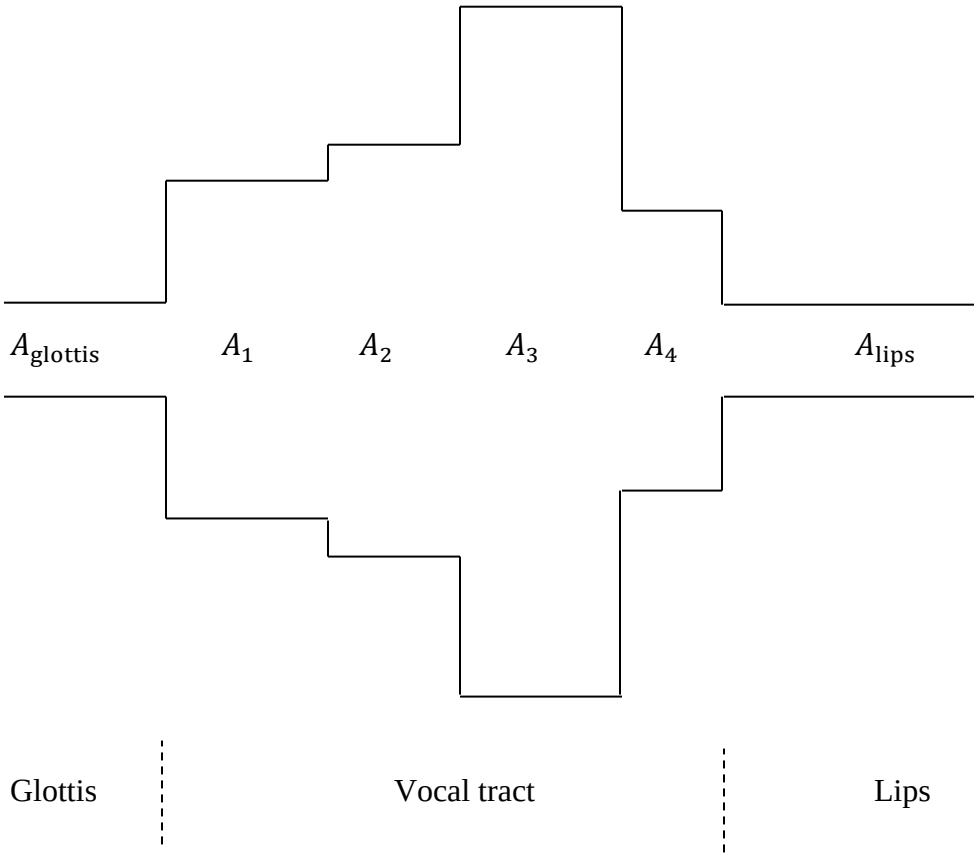

Figure 3.5 Acoustic tube model of vocal tract

With discrete-time processing $H(e^{j\omega})$, formants and a vocal tract consisting of $2n$th order concatenated tubes can be modeled by the multiplication of n second-order infinite impulse response (IIR) resonance filters

$$H(e^{j\omega}) = H_1(e^{j\omega})H_2(e^{j\omega})\cdots H_i(e^{j\omega})\cdots H_n(e^{j\omega}) \quad (3.7)$$

where

$$H_i(e^{j\omega}) = \frac{1}{(1 - p_i e^{-j\omega})(1 - p_i^* e^{-j\omega})}$$

and p_i, p_i^* determine the location of a resonance frequencies F_i in the discrete-time frequency domain of $H(e^{j\omega})$. As the impulse response of vocal tract $H(e^{j\omega})$ is always a BIBO stable system, we have $|p_i|$, $|p_i^*| < 1$. Moreover, $H_i(e^{j\omega})$ can be be expressed as

$$H_i(e^{j\omega}) = \frac{1}{1 - 2|p_i| \cos \angle p_i \cdot e^{-j\omega} + |p_i|^2 e^{-j2\omega}} . \quad (3.8)$$

Then the impulse response corresponding to $H_i(e^{j\omega})$ is

$$h_i[n] = (\sin \angle p_i)^{-1} \cdot |p_i|^{n-2} \cdot \sin \angle p_i (n-1) \cdot u[n-1] .$$

The magnitude $|p_i|$ determines the decreasing rate of $h_i[n]$, and the angle $\angle p_i$ determines the frequency of modulated sinusoidal wave. So a resonance frequency F_i can be shown as

$$F_i = \left(\frac{f_s}{2\pi}\right) \angle p_i$$

where f_s is the sampling frequency for the observed continuous-time speech signal. Then $h_i[n]$ can be re-expressed as

$$h_i[n] = (\sin \omega_i)^{-1} \cdot |p_i|^{n-2} \cdot \sin \omega_i (n-1) \cdot u[n-1]$$

where $\omega_i = 2\pi F_i / f_s$ is the radian frequency of F_i.

If conjugate pole pairs are assumed to be separated far enough from one another, fairly good estimates of bandwidth of a single resonance frequency shown in Figure 2.4 can be represented using

$$\hat{B}_i = \left(\frac{f_s}{\pi}\right) \ln|p_i| .$$

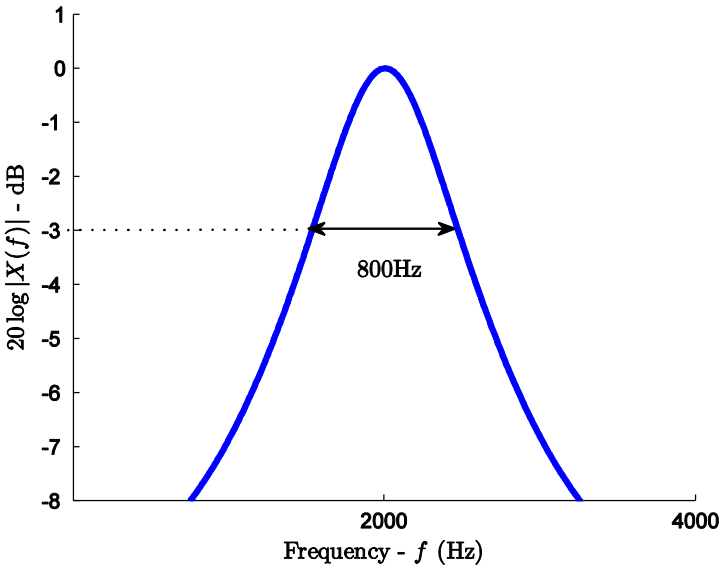

Figure 3.6 Illustration of -3 dB bandwidth between two dot lines for a resonance frequency at 2,000 Hz

With the multiplication effect of responses of a variety of resonance frequencies, the overall frequency response of the vocal tract, $H(e^{j\omega})$, is formed to be a spectral shaping transfer function with conjugate pole pairs contributed from n second-order IIR filter sections whose frequency response can be expressed as

$$H(e^{j\omega}) = \frac{1}{\prod_{1 \le i \le n}(1 - p_i e^{-j\omega})(1 - p_i^* e^{-j\omega})} \tag{3.9}$$

The peaks as a result of resonance poles become the primary features of this all-pole model. If poles $\{p_i, p_i^*\}$, $1 \le i \le n$ are fixed, then $H(e^{j\omega})$ can be found.

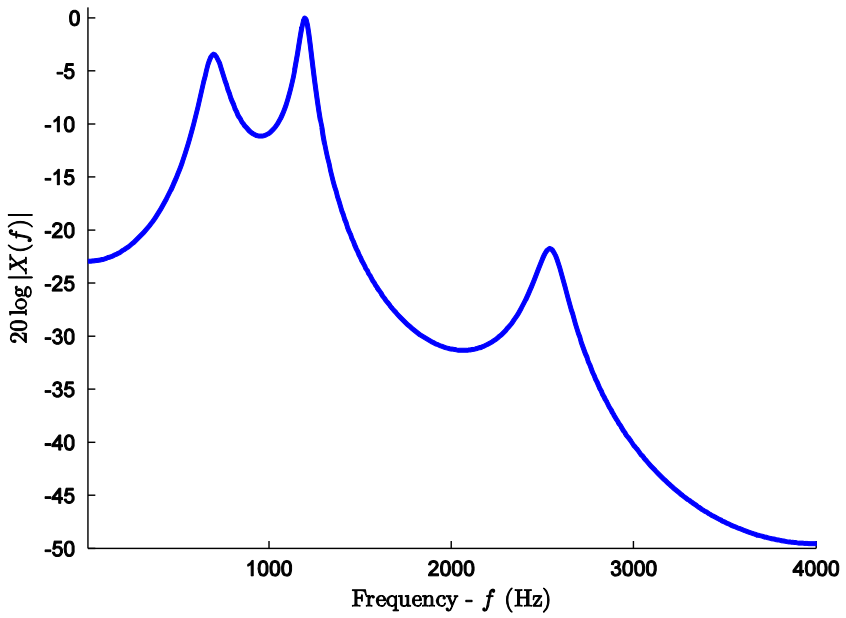

Figure 3.7 Resonance frequencies of a speaker's vocal tract

Though often represented as an all-pole model, the vocal tract can also be characterized by pole-zero models with the introduction of zeros due to the nasal cavity which is involved in the production of some speech sounds [17].

Lips radiation modeled as the first-order difference equation

$$y[n] = x[n] - \alpha x[n-1]$$

where $\alpha < 1$ is often combined with the vocal tract to denote a minimum-phase system because all zeros and poles of these two parts are inside the unit circle. Glottal source, vocal-tract and lips radiation are the three elements in the process of human speech production from the above analysis.

Source-Filter Model for Speech Production

Now we are all set to discuss a complete model about speech production: the source-filter model. This model serves as the key of many speech analysis methods and applications.

Fant [1] considered that the human speech signal can be regarded as the output of a system where the excitation signal is filtered by harmonics at resonance frequencies of the vocal tract. This model is based on the hypothesis that the operation of acoustic dynamics for the overall system is linear and there is no coupling or interaction between source and the vocal tract. Time invariance is assumed. This system basically consists of three independent blocks: periodic or non-periodic excitations (source), the vocal tract (filter) and the effect of lips radiation.

The periodic excitations are caused by the vocal folds' quasi-periodic vibrations. Vowels can be considered as results of this sort of excitations. But the non-periodic excitations are noises occurring when air is forced past a constriction. The transfer function of vocal tract $H(j\Omega)$ behaves as a spectral shaping function affecting the glottal source $U_g(j\Omega)$. So the observed speech signal can be represented by

$$S(j\Omega) = U_g(j\Omega)H(j\Omega)R(j\Omega)$$

where $R(j\Omega)$ denotes the lips radiation response. The above expression provides us a frequency domain relation among these important blocks involved in the speech production process.

A general discrete-time speech production model was proposed in 1978 by Rabiner and Shafer [18]. It deems that any speech utterance can be represented by linear convolution of glottal source, vocal tract and lips radiation shown in Figure 3.8. For discrete-time version this model can be represented as

$$S(e^{j\omega}) = U_g(e^{j\omega})H(e^{j\omega})R(e^{j\omega}) \tag{3.10}$$

It can be expanded as

$$S(e^{j\omega}) = \frac{A(1-\alpha e^{-j\omega})}{\prod_i (1-p_i e^{-j\omega})(1-p_i^* e^{-j\omega})} \cdot U_g(e^{j\omega}) \tag{3.11}$$

The glottal source $U_g(e^{j\omega})$ represents white noise for unvoiced sounds and the periodic glottal pulses for voiced sounds.

The time-domain response of the corresponding speech signal can be represented as

$$s[n] = (u_g * h * r)[n] \tag{3.12}$$

where $s \overset{\mathcal{F}}{\longleftrightarrow} S$, $u_g \overset{\mathcal{F}}{\longleftrightarrow} U_g$, $h \overset{\mathcal{F}}{\longleftrightarrow} H$ and $r \overset{\mathcal{F}}{\longleftrightarrow} R$. The convolution relation in (3.12) as a linear operation provides a way to decompose the observed speech signal and find parameters to estimate signal components using digital techniques. The glottal source signal $u_g[n]$, if it is not noise, can be recovered from the observed speech signal $s[n]$ by applying deconvolution. This process uses estimate of the vocal tract $h[n]$ response modeled as an all-pole model and lips radiation $r[n]$ modeled as a first-order difference equation with parameter $0.98 \leq \alpha < 1$. Properties and assumptions about glottal models discussed in this chapter are based on the work of [1].

Given the overall discrete-time model of speech production in Figure 3.8, consisting of glottal flow pulses models, all-pole and first-order difference for lips radiation, we are able to apply digital signal processing techniques to produce a voiced speech utterance using the glottal models introduced previously and recover glottal flow

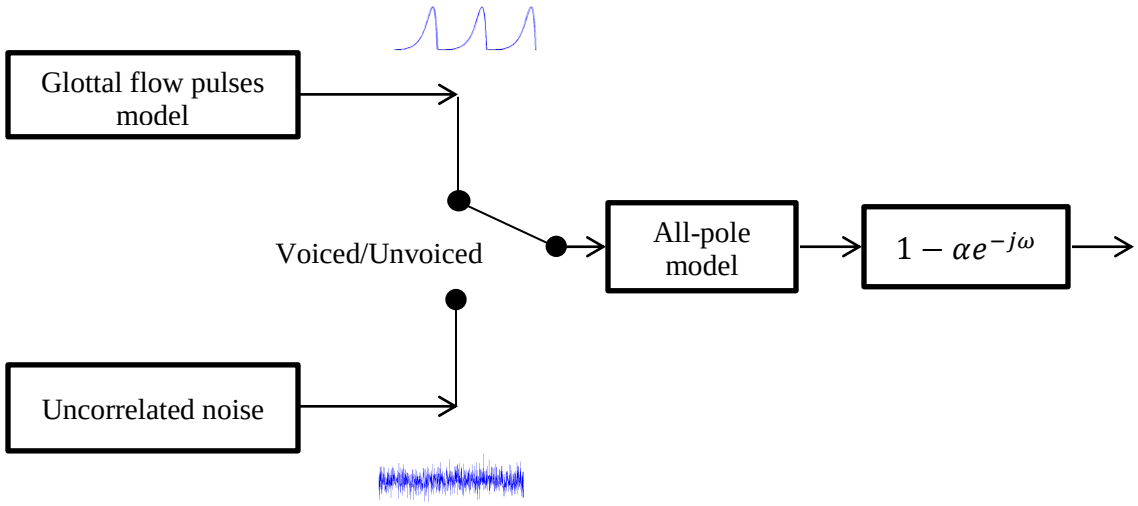

Figure 3.8 The discrete-time model of speech production

pulses whose information is embedded in the waveforms of observed human speech sounds. These discrete-time signal processing techniques including linear prediction and phase separation are core aspects of the algorithms used to estimate glottal pulses in next chapter.

CHAPTER FOUR

THE ESTIMATION OF GLOTTAL SOURCE

This chapter is devoted to details involved in existing methods to extract glottal waveforms of flow pulses. All these methods can be categorized into two classes: those based on parametric models and those that are parameters free. Linear prediction is a major tool for those belonging to the first class. The latter depends on homomorphic filtering to implement phase decomposition as well as glottal closure instants (GCI) detection to determine the data analysis region.

Two Methods of Linear Prediction

Until very recently, the linear prediction based methods have dominated the task of building models to find the glottal flow pulses waveform [20], [21], [22] for different speakers. Normally, either an estimator based on the second order statistics or an optimization algorithm is required to find the best parameters in statistical and optimization senses with respect to the previously chosen model. Two methods, the autocorrelation method and the covariance method [23], are available to estimate the parametric signal model in the minimum-mean-square estimation (MMSE) sense and the least-squares estimation (LSE) sense, respectively. The autocorrelation method assumes the short-time wide sense stationarity of human speech sounds to set up the Yule-Walker equation set.

Given a p th-order linear predictor and an observed quasi-stationary random vector $\{X_0, X_1, \cdots, X_p\}$ sampled from a speech signal $X(t)$, a residual error signal w_p is

defined as

$$w_p = X_p - \sum_{i=1}^{p} a_i X_{p-i}\,. \tag{4.1}$$

Then a MMSE problem can be formulated as

$$\underset{\mathbf{a}=\{a_1,a_2,\cdots,a_p\}}{\arg\max}\ \mathbb{E}\left|X_p - \hat{X}_p\right|^2 \tag{4.2}$$

where

$$\hat{X}_p = \sum_{i=1}^{p} a_i X_{p-i} \tag{4.3}$$

from which we obtain the coefficient vector **a** of the predictor by solving the problem represented by (4.2). From (4.1) we have Yule-Walker equations which have the form:

$$\mathbf{\Gamma}_X \mathbf{a} = \mathbf{r} \tag{4.4}$$

where

$$\mathbf{\Gamma}_X = \begin{bmatrix} R_X(0) & \cdots & R_X(p-1) \\ \vdots & \ddots & \vdots \\ R_X(p-1) & \cdots & R_X(0) \end{bmatrix}$$

denotes the autocorrelation matrix of X_i, $0 \le i \le 2N-1$, and $\mathbf{r} = [\sigma_w, 0, \cdots, 0]^T$, where σ_w is the square root of the residual error's power. $R_X(\cdot)$ is the autocorrelation function for the signal $X(t)$, The correlation $\mathbb{E}\, X_{2N-\ell} X_{2N-\hbar}$, $0 \le \ell, \hbar \le 2N-1$ can be estimated by an average estimator

$$\mathbb{E}\, X_{p-\ell} X_{p-\hbar} \cong \frac{1}{2N} \langle \mathbf{x}^{(\ell)}, \mathbf{x}^{(\hbar)} \rangle \tag{4.5}$$

where $\mathbf{x}^{(\ell)}$ and $\mathbf{x}^{(\kappa)}$ denote ℓ-unit and κ-unit right shift of $\mathbf{x}$. Levinson Recursion is able to efficiently find the optimum solution $\mathbf{a}^*$ of the Yule-Walker equation set in the MSEE sense.

In the autocorrelation method, the order of linear prediction fixes the dimension of the Toeplitz matrix $\mathbf{\Gamma}_X$. It gives a rise to fairly large error since the order of the predictor can't be high. Additionally, since the autocorrelation method just minimizes the mean-square error and requires strong stationarity for a fairly accurate second order statistical result, it has limitations to achieving the good performance in some environments if it is compared with the covariance method [23].

The covariance method is based on linear least-squares regression of linear equations without relying on any statistical feature of the observed sequence. To set up its own data matrix, the acquisition of observed data is realized by an analysis window on the objective speech signal. As in the autocorrelation method, the dimension of columns is uniquely determined by the order of linear prediction. But the dimension of rows for the covariance method depends on the number of shift positions of linear predictor inside the external analysis window. The number of rows is often larger than that of columns.

Given a pth-order linear predictor and a length-N analysis window of random vector $\mathbf{x} = [X_0\, X_1\, \cdots\, X_{N-1}]^T$ sampled from a speech signal $X(t)$, by shifting the predictor inside the window we can form an data matrix $\widetilde{\mathbf{X}}$ which leads to solving a problem of the form $\hat{\mathbf{x}} = \widetilde{\mathbf{X}}\mathbf{a}$ by a variety of windowing ways. Here $\widetilde{\mathbf{X}} \in \mathbb{R}^{N\times p}$ is an over-determined system with rank r that might not equal to N or p. That is, $\widetilde{\mathbf{X}}$ can be a rank-

deficient matrix. A LSE problem to minimize the ℓ^2-norm of $\|\mathbf{x} - \hat{\mathbf{x}}\|$ can be formulated as

$$\underset{\mathbf{a}}{\operatorname{argmin}} \left\| \mathbf{x} - \widetilde{\mathbf{X}}\mathbf{a} \right\| \tag{4.6}$$

There exists a method of algorithms to solve above over-determined least-squares problem. One option is to employ Singular Value Decomposition (SVD) in its computation [24].

The minimum ℓ^2-norm can also be found by decomposing $\widetilde{\mathbf{X}}$ shown as [25]

$$\left\| \mathbf{x} - \widetilde{\mathbf{X}}\mathbf{a} \right\| = \|\mathbf{x} - \mathbf{U}\boldsymbol{\Sigma}\mathbf{V}^T\mathbf{a}\| = \|\mathbf{U}^T\mathbf{x} - \boldsymbol{\Sigma}\mathbf{V}^T\mathbf{a}\| \tag{4.7}$$

where $\boldsymbol{\Sigma}$ contains singular values of $\widetilde{\mathbf{X}}$ and $\mathbf{U} \in \mathbb{R}^{N\times N}, \mathbf{V} \in \mathbb{R}^{p\times p}$ are orthogonal matrices with $\mathbf{U} = [\mathbf{u}_1\ \mathbf{u}_2\ \cdots\ \mathbf{u}_N]$ and $\mathbf{V} = \left[\mathbf{v}_1\ \mathbf{v}_2\ \cdots\ \mathbf{v}_p\right]$. That is, $\mathbf{U}\mathbf{U}^T = \boldsymbol{I}$ and $\mathbf{V}\mathbf{V}^T = \boldsymbol{I}$. Let $\mathbf{x}' = \mathbf{U}^T\mathbf{x}$ and $\mathbf{a}' = \mathbf{V}^T\mathbf{a}$ be projections of **x** and **a;** then we can obtain another equivalent expression

$$\underset{\mathbf{a}'}{\operatorname{argmin}} \|\mathbf{x}' - \boldsymbol{\Sigma}\mathbf{a}'\| \tag{4.8}$$

where

$$\|\mathbf{x}' - \boldsymbol{\Sigma}\mathbf{a}'\|^2 = \sum_{i=1}^{r} |x_i' - \sigma_i a_i'|^2 + \sum_{i=r+1}^{N} |x_i'|^2$$

which is minimized if and only if $a_i' = x_i' / \sigma_i = \mathbf{u}_i^T\mathbf{x} / \sigma_i$ for $1 \le i \le r$ and $a_i' = 0$ for $r + 1 \le i \le M$. The least-squares solution $\mathbf{a}^*$ is

$$\mathbf{a}^* = \sum_{i=1}^{r} \left(\frac{\mathbf{u}_i^T\mathbf{x}}{\sigma_i} \right) \mathbf{v}_i$$

or

$$\mathbf{a}^* = \widetilde{\mathbf{X}}^{+}\mathbf{x}$$

where $\widetilde{\mathbf{X}}^{+} = \sum_{i=1}^{r}(\mathbf{v}_i\mathbf{u}_i^T/\sigma_i)$ is the pseudo-inverse of $\widetilde{\mathbf{X}}$.

The determination of the rank of a low dimensional matrix is easy theoretically, but it becomes more complicated in practical applications. The conventional recursive least-squares (RLS) algorithm has been the major tool for speech processing implementations since there doesn't exist special consideration about the rank of $\widetilde{\mathbf{X}}$. The overall procedure can be summarized as below [25], [26]

i. Initialize the coefficient vector and the inverse correlation matrix by $\mathbf{a}(-1) = 0$ and $\mathbf{P}(-1) = \lambda\mathbf{I}$ where λ is the forgetting factor.

ii. $\forall\, n = 0,1,\ldots,L-1$, where L is the length of the analysis window using

$$\begin{cases} \bar{\mathbf{g}}_\lambda(n) = \mathbf{P}(n-1)\tilde{\mathbf{x}}(n) \\ \alpha_\lambda(n) = \lambda + \bar{\mathbf{g}}_\lambda^H(n)\tilde{\mathbf{x}}(n) \end{cases}$$

we can compute the adaptation gain and update the inverse correlation matrix

$$\mathbf{g}(n) = \frac{\bar{\mathbf{g}}_\lambda(n)}{\alpha_\lambda(n)}$$

and

$$\mathrm{P}(n) = \lambda^{-1}\left[\mathbf{P}(n-1) - \mathbf{g}(n)\bar{\mathbf{g}}_\lambda^T(n)\right]$$

iii. Filter the data and update coefficients

$$\mathrm{e}(n) = \mathrm{x}(n) - \mathbf{a}^T(n-1)\tilde{\mathbf{x}}(n)$$

and

$$\mathbf{a}(n) = \mathbf{a}(n-1) + \mathrm{e}(n)\mathbf{g}(n)\,.$$

There are other versions [27], [28] of RLS algorithms used for the covariance method to solve (4.7).

The autocorrelation method of MMSE has low computation costs to solve Yule-Walker equations; however, the RLS method involves more computational costs. And it has been proven to have better performance on voiced signals than autocorrelation method [29]. Basically, the covariance method is considered as a pure optimization problem; however, the autocorrelation method works on second-order statistics. These two methods share a mutual characteristic: the model type and order for linear prediction. For the covariance method, the length of the analysis window should be known as a priori information.

In some cases, we need other methods, which don't rely on any a priori information of the given signal, to process the speech signal and extract the information of interest.

Homomorphic Filtering

Suppose an observed sequence $x[n]$ is the output of a system $h[n]$ excited by a sequence $e[n]$ as represented by

$$x[n] = (h * e)[n]$$

We have

$$\ln X(e^{j\omega}) = \ln|X(e^{j\omega})| + j\measuredangle X(e^{j\omega})$$

which will result in phase discontinuities in the principal value of the phase at $\omega = \pm\pi$ if there exists a linear phase response in $X(e^{j\omega})$.

From another viewpoint, let $x[n] \overset{\mathcal{F}}{\longleftrightarrow} X(e^{j\omega})$, $h[n] \overset{\mathcal{F}}{\longleftrightarrow} H(e^{j\omega})$ and $e[n] \overset{\mathcal{F}}{\longleftrightarrow} E(e^{j\omega})$, then the logarithm can be applied to $X(e^{j\omega})$ to separate logarithm transformations of $H(e^{j\omega})$ and $E(e^{j\omega})$ as

$$\ln X(e^{j\omega}) = \ln H(e^{j\omega}) + \ln E(e^{j\omega}) \tag{4.9}$$

The cepstral relation can be obtained

$$\hat{c}_x(\tau) = \hat{c}_h(\tau) + \hat{c}_e(\tau) \tag{4.10}$$

where $\hat{c}_x(\tau) \overset{\mathcal{F}}{\longleftrightarrow} \ln X(e^{j\omega})$, $\hat{c}_h(\tau) \overset{\mathcal{F}}{\longleftrightarrow} \ln H(e^{j\omega})$ and $\hat{c}_e(\tau) \overset{\mathcal{F}}{\longleftrightarrow} \ln E(e^{j\omega})$. Based on this relation, the linear deconvolution of $h[n]$ and $e[n]$ can be implemented. If $\hat{c}_h(\tau)$ and $\hat{c}_e(\tau)$ are not overlapped in the quefrency domain, then a "lifter" can be used to separate these two cepstral representations. The deconvolution in the homomorphic domain provides a way to discriminate a glottal-excitation response and a vocal-tract response if their cepstral representations are separable in the quefrency domain [13], [19]. Note: phase unwrapping is used to compensate for the issue of phase discontinuities, as described in chapter 5.

Glottal Closure Instants Detection

In terms of voiced speech, the major acoustic excitation in the vocal tract usually occurs at instants of vocal-fold closure defined as the glottal closure instants. Each glottal closure indicates the beginning of the closed phase, during which there is little or no glottal airflow through the glottis, of the volume velocity of the glottal source. The

detection of glottal closure instants plays an important role in extracting glottal flow pulses synchronously and tracking the variation of acoustic features of speakers.

Automatic identification of glottal closure instants has been an important topic for speech researchers in the past two decades. Because the measured speech signal is the response of the vocal tract to the glottal excitation, it is a challenge to perform accurate estimation of these instants in a recorded speech utterance.

Many methods have been proposed about this topic. A widely used approach is to detect a sharp minimum in a signal corresponding to a linear model of speech production [30], [31]. In [30], the detection of glottal closure instants is obtained by the lower ratio between residual errors and original signal after the linear prediction analysis is applied to a speech utterance. Group delay measures [30], [32] can be another method to determine these instants hidden in the observed voiced speech sounds. They estimate the frequency-averaged group delay with a sliding window on residual errors after linear prediction. An improvement was achieved by employing a Dynamic Programming Projected Phase-Slope Algorithm (DYPSA) [31]. Best results come from analysis on the differentiated Electroglottograph (EGG) [33] (or Laryngograph signal [34]) from the measurement of the electrical conductance of the glottis captured during speech recordings. However, good automatic GCI detection methods with better estimations have a high computation cost.

Parametric Approaches to Estimate Glottal Flow Pulses

Applications of covariance analysis to the problem of extraction of glottal flow pulses have been performed successfully for short voiced phoneme utterances by some researchers [20], [21]. All parametric estimation methods to extract glottal flow pulses have three components: application of linear prediction analysis, normally using the covariance method; selection of the optimum linear prediction coefficients set to represent the vocal-tract response; and deconvolution of the original speech using estimated linear prediction coefficients to extract glottal flow pulses.

Wong, Markel and Gray proposed the first parametric approach [21] using covariance analysis. Their approach can be summarized as follows. Assume an all-pole model $H(z)$ for the vocal-tract and fix the model order. The size of an analysis frame is selected to ensure that the sliding window has all data needed between the two ends of the analysis frame. Then set up an over-determined system using data inside all sliding windows and employ the least square algorithm to find the optimum parameters. Then the parameter set and the ℓ^2 -norm of the residual error vector are both recorded corresponding to the current specific location of the sliding window. Finally, access the recorded parameters corresponding to the location where the power ratio between residual errors and the original signal is minimized. Consequently, that chosen parameter set is used to form the inverse system of the vocal-tract model, through which the inverse filtering for deconvolution is applied to the original speech sequence. The result of the operation is the combination of the glottal pulse and lips radiation. Furthermore, we can estimate the glottal pulse waveform by removing lips radiation $R(z)$ from the overall

response of the speech utterance denoted by $S(z)$. The procedure for estimating the glottal pulse $p[n]$ is described by

$$p[n] = \mathcal{Z}^{-1}\{S(z)H^{-1}(z)R^{-1}(z)\}. \tag{4.11}$$

The mismatch of locating the glottal closure phase estimated as above will introduce inaccuracies to the final estimation of pulses.

Alku proposed another method [4], iterative adaptive inverse filtering (IAIF), to extract glottal flow pulses by two iterations. It requires a priori knowledge about the shape of the vocal tract transfer function which can be firstly estimated by covariance analysis of linear prediction after the tilting effect of glottal pulse in frequency domain has been eliminated from the observed speech. In the first iteration, the effect of the glottal source estimated by a first-order linear prediction all-pole model was used to inverse filter the observed speech signal. A higher-order covariance analysis was applied to the resulting signal after inverse filtering. Then a second coarse estimate is obtained by integration to remove the lips radiation from last inverse filtering result. Another two rounds of covariance analysis are applied in a second process. Correspondingly, two inverse-filtering procedures are involved in the whole iteration. A refined glottal flow pulse is estimated after another stage of lips radiation cancellation. Compared with the previous method, an improvement in the quality of estimation has been achieved with a sophisticated process, in which four stages of linear prediction have been used.

In addition to these two approaches based on all-pole models, there are other approaches based on different model types [22]. Using a priori information about model type and order, these parametric methods can estimate and eliminate the vocal-tract

response. However, the number of resonance frequencies needed to represent a specific speaker and his pronounced phonemes is unknown. This uncertainty about orders of the all-pole model might largely affect the accuracy of the estimation of the vocal-tract response. Some researchers found another way to extract the glottal excitations to circumvent these uncertainties about linear prediction models. These are summarized below.

Nonparametric Approaches to Estimate Glottal Flow Pulses

The LF model has been widely accepted as a method for representing the excitation for voiced sounds since it contains an asymptotically closing phase to correspond to the activity of speaker's closing glottis.

The LF model's closed and open phases have been shown to consist of contributions by maximum-phase components [13]. The LF model offers an opportunity to use nonparametric models to recover an individual pulse. Meanwhile, a linear system's phase information becomes indispensable in the task of glottal pulse estimation. The Zeros of $\mathcal{Z}$-transform (ZZT) method and the complex cepstrum (CC) method [19], [20] have been applied to the speech waveform present within one period of vocal-folds between closed phases of two adjacent pulses. Then maximum-phase and minimum-phase components can be classified as the source (glottal pulse) and tract (vocal-tract) response, respectively. For nonparametric approaches the vocal tract is considered to be contributing only to the minimum-phase components of the objective sequence. And maximum-phase components correspond to the glottal pulse.

It has been recognized that human speech is a mixed-phase signal where the maximum-phase contributions corresponds to the glottal open phase while the vocal tract component is assumed to be minimum-phase. The "zeros of the $\mathcal{Z}$-transform" method [19] technique can be used to achieve causal and anti-causal decomposition.

It has been discussed that the complex cepstrum representation can be used for source-tract deconvolution based on pitch-length duration with glottal closure as its two ends. But there are some weaknesses in terms of nonparametric methods as discussed below.

The pinpoint of the two instants to fix the analysis region will be necessary for all these existing nonparametric methods. Although there have been some glottal closure instants detection algorithms proposed, selecting the closed phase portion of the speech waveform has still been a challenge to ensure the high-quality glottal closure instants detection. This adds computational costs to the estimation of glottal flow pulses. On the other hand, the minimum-phase and maximum-phase separation assumes the finite-length sequence is contributed by zeros which contradicts the fact that vocal-tract response is usually regarded as the summation of infinite attenuating sinusoidal sequences that might be longer than one pitch.

Any finite-length speech utterance $x[n]$ can be viewed as the impulse response of a linear system containing both maximum-phase and minimum-phase components. The $\mathcal{Z}$-transform of the signal can be represented as

$$X(z) = \frac{A \cdot \prod_k (1 - \alpha_k z^{-1}) \prod_n (1 - \beta_n z) z^{-\ell}}{\prod_i (1 - p_i z^{-i})(1 - p_i^* z^{-i})} \tag{4.12}$$

where $\{\alpha_k\}, \{\beta_n\}, \{p_i, p_i^*\}$ all have magnitude less than one and $z^{-\ell}$ is the linear phase terms as the result of maximum-phase zeros.

With the homomorphic filtering operation, the human speech utterance as a system response can be separated into maximum and minimum phase components. The factors of $X(z)$ are classified into time-domain responses contributed by maximum-phase and minimum-phase components. Then both maximum-phase and minimum-phase parts can be separated by calculating the complex cepstrum $\hat{x}[n]$ of the speech signal $x[n]$ during adjacent vocal fold periods. As we indicated before, pitch detection will be needed to ensure those two types of phase information can be included in the analysis window.

Summary

In this chapter, we summarized both parametric and nonparametric methods involving linear prediction, homomorphic filtering, and GCI detection to estimate glottal flow pulses from a voiced sound excited by periodic glottal flow pulses. However, these two major classes of methods have their own weaknesses caused by the characteristics of these respective processing schemes. These weaknesses sometimes can largely reduce the accuracies of the estimation of pulses and introduce distortions to them. For the remaining chapters, the challenge confronting us changes from extracting excitation pulses to preserving recognizable features of pulses with the largest possible fidelity.

CHAPTER FIVE

JOINTLY PARAMETRIC AND NONPARMETRIC ESTIMATION APPROACHES OF GLOTTAL FLOW PULSES I

Linear prediction and complex cepstrum approaches have been shown to be effective for extracting glottal flow pulses. However, all of these approaches have their limited effectiveness. After the weaknesses of both parametric and nonparametric methods [17], [18], [19] presented had been considered seriously, a new hybrid estimation scheme is proposed in this chapter. It employs an odd-order LP analyzer to find parameters of an all-pole model by least-squares methods and obtains the coarse GFP by deconvolution. It then applies CC analysis to refine the GFP by eliminating the remaining minimum-phase information contained in the glottal source estimated by the first step.

Introduction

We present here a jointly parametric and nonparametric approach to use an odd-order all-pole predictor to implement the LP analysis. Covariance methods of linear prediction analysis typically based on all-pole models representing the human vocal tract once dominated the task of glottal pulse extraction [20], [21]. They adapted a least-square optimization algorithm to find parameters for their models given the order of models, and the presence or absence of zeros. These models with a priori information involve strong assumptions, which ignore some other information that might be potentially helpful for more accurate separation.

The introduction of the residual errors from LP analysis, normally regarded as Gaussian noise, affects the glottal pulse extraction results. On the other hand, an individual LF model [10], [12] has a return phase corresponding to the minimum-phase components [19]. The return phase can recovered by polynomial roots analysis. This method can be used to perform decomposition of the maximum-phase part and minimum-phase part of speech signals. Decomposition results have proven helpful for achieving the source-tract separation. The decompositions are carried out on a finite-length windowed speech sequence where the window end points are set to the glottal closure instants [19], [35]. ZZT and CC, which involve polynomial factorization are effective for the decomposition in terms of the phase information of the finite-length speech sequence. There are two factors that might affect the final separation results. The finite number of zeros might be insufficient to represent the vocal tract. Also, accurate detection of GCIs involves high computation costs.

If the vocal-tract is not lossless [17], it is assumed to be minimum-phase and represented by complex conjugate poles of an all-pole model. Any individual glottal pulse is forced to be represented using at least one real pole from the model.

Based on the above consideration, we refined previous separation results using the CC to realize the phase decomposition. Simulation results shown later in this chapter demonstrate that, compared with existing parametric and nonparametric approaches, the presented approach has better performance to extract the glottal source.

The vocal-tract is assumed to be a minimum-phase system represented by complex conjugate poles of an all-pole model. With extending the covariance analysis

window, the variance coming from different locations of the window will be largely reduced as Figure 5.1 shows. We can therefore utilize the covariance methods in the normal LP analysis applications free of sensitive location of the window [36], [37]. Therefore, any individual glottal pulse is forced to be represented using at least one real pole in the LS regression process. Then we refined separation results with CC to realize the phase decomposition.

Based on the estimated performance for both synthetic and real speech utterances, our simulation results demonstrate, like existing completely parametric and nonparametric approaches, that the presented approach also has effective and promising performance to extract the glottal flow pulses. Additionally, the new approach won't consume much computational resource.

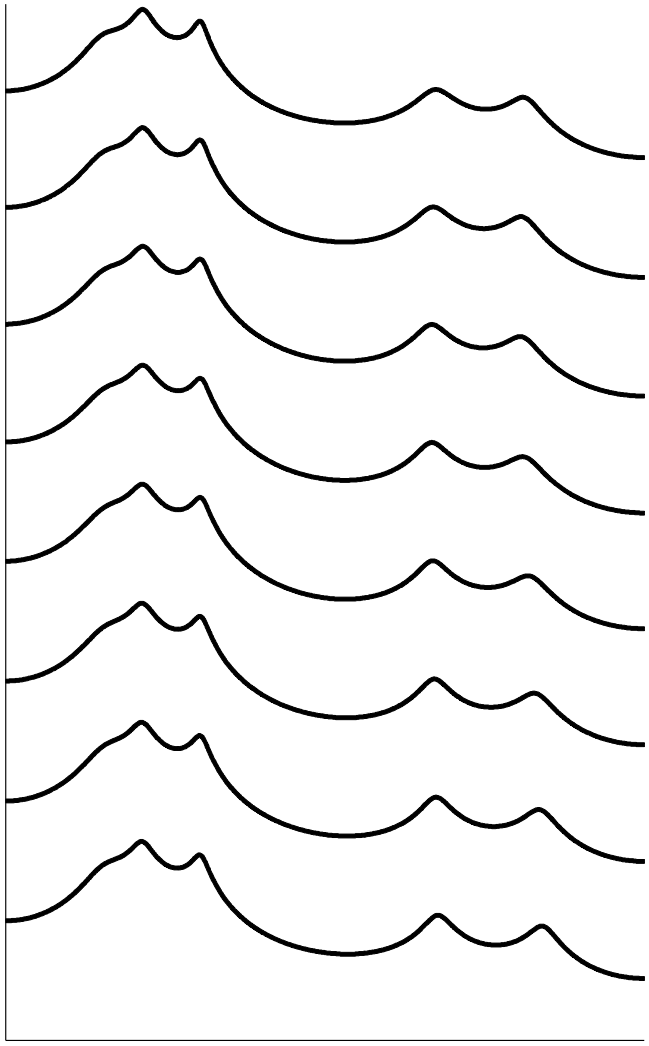

Figure 5.1 Illustration of vocal-tract response from linear prediction analysis with overlapped Blackman windows

Odd-Order Linear Prediction Preprocessing and Inverse Filtering

Consider the voiced speech signal $\mathbf{x}[n]$ for which the $\mathcal{Z}$-transform is denoted by

$$X(z) = G(z)H(z) \tag{5.1}$$

where $G(z)$ is response of glottal flow pulses (GFPs) and the lip radiation, and $H(z)$ is the response of vocal tract that is a minimum-phase system and it might contain zeros. $H(z)$ can be represented by

$$H(z) = H_{az}(z)H_{ap}(z)\,.$$

Here $H_{az}(z)$ denotes all-zero part and $H_{ap}(z)$ denotes all-pole part of the vocal-tract response. The determination of $G(z)$ and $H(z)$ leads to the source-tract separation.

Covariance methods of LP analysis, usually with even order, have become a major tool for the parametric analysis of voiced speech utterances. On the other hand, an odd-order all-pole model expressed by

$$\widehat{H}_{ap}(z) = \frac{1}{1 - \sum_{m=1}^{2M+1} a_m z^{-m}}$$

guarantees that at least one real pole is included to represent the low-pass tilting effect of the glottal source. We can separate $\widehat{H}_{ap}(z)$ into two systems $\widehat{H}_{ap\_comp}(z)$ contributed by complex pole pairs and $\widehat{H}_{ap\_real}(z)$ contributed by real poles.

Let $\mathbf{x}_n = \left[x_1^{(n)}, \ldots, x_N^{(n)}\right]^T \in \mathbb{R}^N$ be a windowed discrete-time speech frame and $\hat{\mathbf{x}}_n = \widetilde{\mathbf{X}}_n \mathbf{a}_n^T$ be the optimum estimate of $\mathbf{x}_n$ in the Least-Squares (LS) sense. Then the all-pole model coefficients vector $\mathbf{a}_n = \left[a_1^{(n)}, \cdots, a_{2M+1}^{(n)}\right]^T$ is found to minimize the ℓ^2 norm error between the observed signal $\mathbf{x}_n$ and its estimate $\hat{\mathbf{x}}_n$. In general,

$$\underset{\mathbf{a}_n}{\operatorname{argmin}} \left\| \mathbf{x}_n - \widetilde{\mathbf{X}}_n \mathbf{a}_n^T \right\| \tag{5.2}$$

where $\widetilde{\mathbf{X}}_n \in \mathbb{R}^{N\times(2M+1)}$ is defined by

$$\widetilde{\mathbf{X}}_n = \begin{bmatrix} x_{-2M}^{(n)} & x_{-2M+1}^{(n)} & \cdots & x_{-1}^{(n)} & x_0^{(n)} \\ x_{-2M+1}^{(n)} & x_{-2M+2}^{(n)} & \cdots & x_0^{(n)} & x_1^{(n)} \\ \vdots & \vdots & \vdots & \vdots & \vdots \\ x_{N-2M-1}^{(n)} & x_{N-2M}^{(n)} & \cdots & x_{N-2}^{(n)} & x_{N-1}^{(n)} \end{bmatrix} \tag{5.3}$$

which is a data matrix formed with a shifted version of the current observation data frame; $\mathbf{x}_n$ and $\hat{\mathbf{a}}_n$ can be determined by recursive LS algorithms.

Given a predictor coefficient vector $\hat{\mathbf{a}}_n$ with odd elements, there exists at least one real root $p_i \in \mathbb{R}$, such that

$$\cdots (1 - p_i z^{-1}) \cdots = 1 - \sum_{m=1}^{2M+1} \hat{a}_m z^{-m}$$

as the result of LS estimation. Then the remaining complex poles $\mathcal{P} \setminus p_i$, excluding p_i from the set $\mathcal{P}$, are reserved for the representation of the coarse vocal-tract response. Here $\mathcal{P}$ is the set of all roots of the above polynomial.

These estimated complex conjugate poles further form a linear filter which can be used to deconvolve the observed speech signal to obtain the coarse representation of the glottal source corresponding to the current speech frame. Thus, it results in the estimated glottal excitation $\mathbf{e}[n] \overset{z}{\longleftrightarrow} E(z)$ expressed by

$$E(z) = \frac{X(z)}{\widehat{H}_{ap\_comp}(z)} = G(z)H_{az}(z)H_{ap\_real}(z) \cdot \Theta(z) \tag{5.4}$$

where $\Theta(z)$ on the right hand side of (7) can be further expressed by

$$\Theta(z) = \frac{H_{ap\_comp}(z)}{\hat{H}_{ap\_comp}(z)} \tag{5.5}$$

which denotes the ratio between $H_{ap\_comp}(z)$ and its estimate $\hat{H}_{ap\_comp}(z)$. Because $|p_i| \leq 1, \forall\, p_i \in \mathcal{P}$, $\hat{H}_{ap\_comp}(z)$ is minimum-phase. The ratio $\Theta(z)$ is a minimum-phase system as well. Therefore, the coarse estimate of GFPs will still be a mixed-phase system affected by cancelling effects of the ratio between $H_{ap\_comp}(z)$ and $\hat{H}_{ap\_comp}(z)$. A new estimate $\mathbf{e}[n]$ can be defined by

$$\mathbf{e}[n] = (\mathbf{p} * \mathrm{g} * \xi)[n] \tag{5.6}$$

where $\mathrm{g}[n]$ is an individual glottal pulse, $\xi[n]$ is the error introduced by the inverse filtering and $\mathbf{p}[n]$ is an impulse train defined by

$$\mathbf{p}[n] = \sum_i \delta[n - iN - \boldsymbol{\theta}] \tag{5.7}$$

with the pitch length N and the random phase distortion $\boldsymbol{\theta}$. This information in $\mathbf{p}[n]$ is much more obvious from the illustration in Figure 5.2 than from the original speech waveforms.

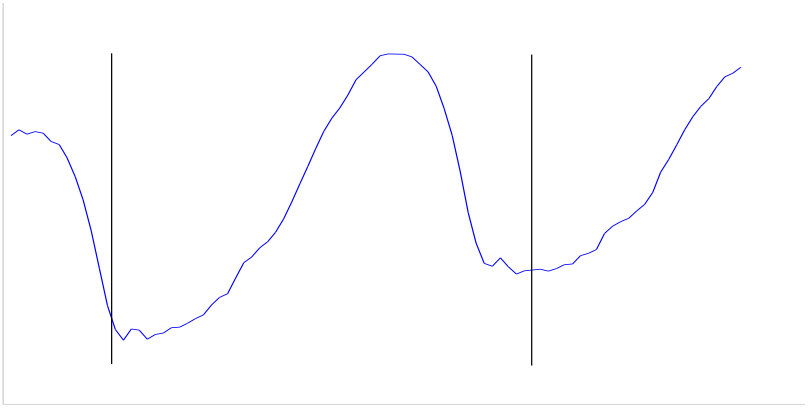

Figure 5.2 Analysis region after LP analysis

This enables us to employ a simpler system to obtain the GFP information using the phase decomposition to extract the minimum phase parts in $\mathbf{e}[n]$ which is mixed-phase.

Phase Decomposition

Results from the covariance method of odd-order LP analysis form a good foundation for further processing. After the inverse filtering, phase decomposition can be used to refine the estimate of the glottal pulse by removing the minimum-phase part. It also can be used for synchronized GFP recovery.

Fixing $\boldsymbol{\theta}$ for each pulse, we are able to detect the glottal closure instants in $\mathbf{e}[n]$ for its pulses' refinements. Let $\tilde{\mathbf{e}}[n]$ be a portion of the glottal excitation $\mathbf{e}[n]$ between two adjacent GCIs and $\tilde{\mathbf{e}}[n] \overset{\mathcal{Z}}{\longleftrightarrow} \tilde{E}(z)$ where

$$\tilde{\mathbf{e}}[n] = (\tilde{\mathbf{e}}_{max} * \tilde{\mathbf{e}}_{min})[n]. \tag{5.8}$$

$\tilde{\mathbf{e}}[n]$ can be analyzed by homomorphic filtering to separate the minimum-phase and maximum-phase sequences. The region between the two solid lines in Figure 5.2 for CC analysis spans slightly longer than one pitch between two GCIs. Notice the tilting effect due to the bias [21].

After phase unwrapping and determination of the algebraic sign of the gain A of $\tilde{E}(z)$, the computation of the finite-length CC of $\tilde{\mathbf{e}}[n]$, which can be regarded as a higher-order polynomial can be performed using [23]

$$\mathcal{Z}^{-1}\{\ln[\tilde{E}(z)]\} = \begin{cases} \ln|A|, \ n = 0 \\ -\sum_m \frac{a_m^n}{n}, n > 0 \\ \sum_k \frac{b_k^{-n}}{n}, n < 0 \end{cases} \tag{5.9}$$

where coefficients a_m and b_k are the polynomial's minimum-phase roots and maximum-phase roots' reciprocals, respectively. The quantities of the cepstrum representation on the left side of the origin contribute to the maximum-phase components of $\tilde{\mathbf{e}}[n]$ for the current pulse. Due to time-domain aliasing, the low-index terms of the maximum-phase components are not taken into account for the following inverse transform to recover the current GFP. As shown in Figure 5.3 round dots for the maximum-phase are reserved as the input for the following operation that converts the response from the cepstrum domain back to the time-domain.

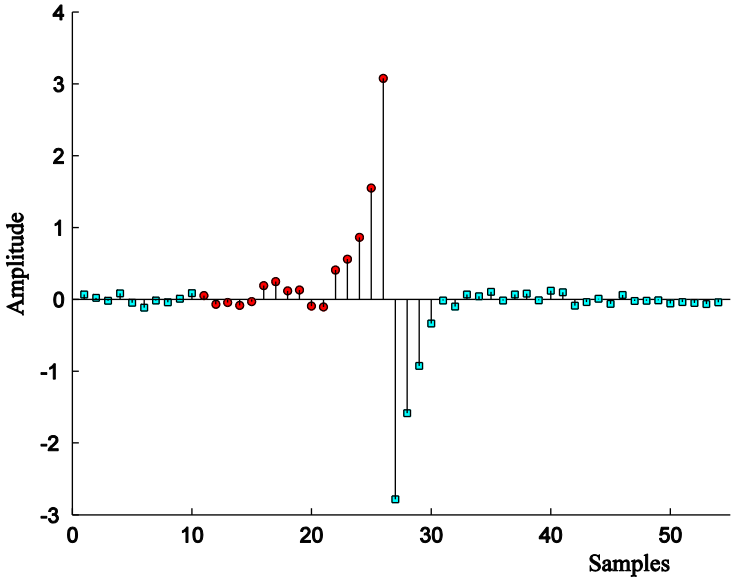

Figure 5.3 Finite-length complex cepstrum of $\tilde{\mathbf{e}}[\boldsymbol{n}]$. (Round dots will be reserved for the inverse transform to recover the pulse.)

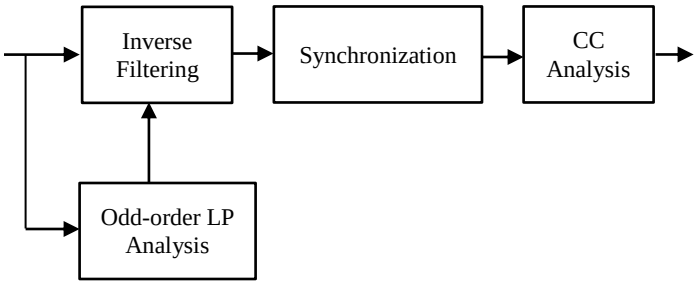

Figure 5.4 The odd-order LP and CC flow (CC analysis consists of $\mathcal{D}_*[\cdot]$, liftering, $\mathcal{D}_*^{-1}[\cdot]$, left-right hand separation where $\mathcal{D}_*[\cdot]$ denotes cepstrum transformation)

Figure 5.4 shows an overall signal flow diagram for the procedures described in this section.

Waveform Simulations

In order to evaluate the performance of the proposed approach in terms of individual GFPs, two sets of experiments with 8 kHz sampling rate were conducted.

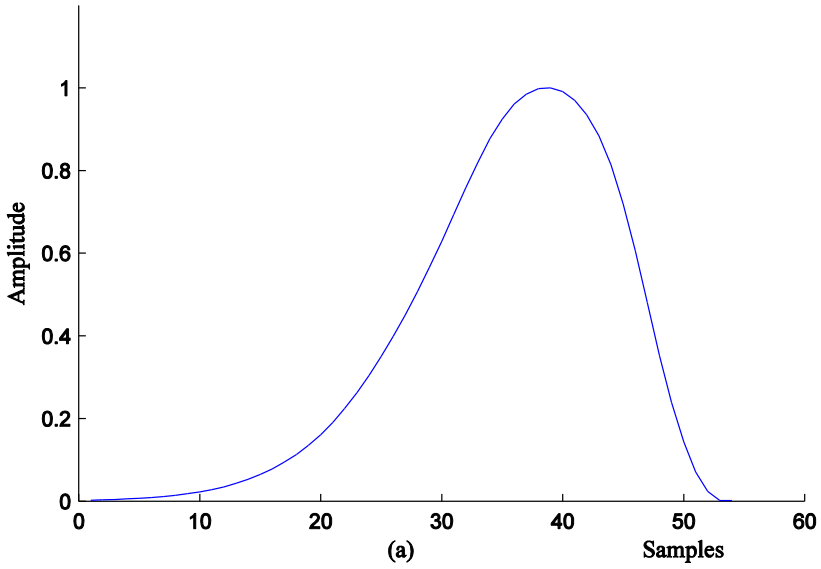

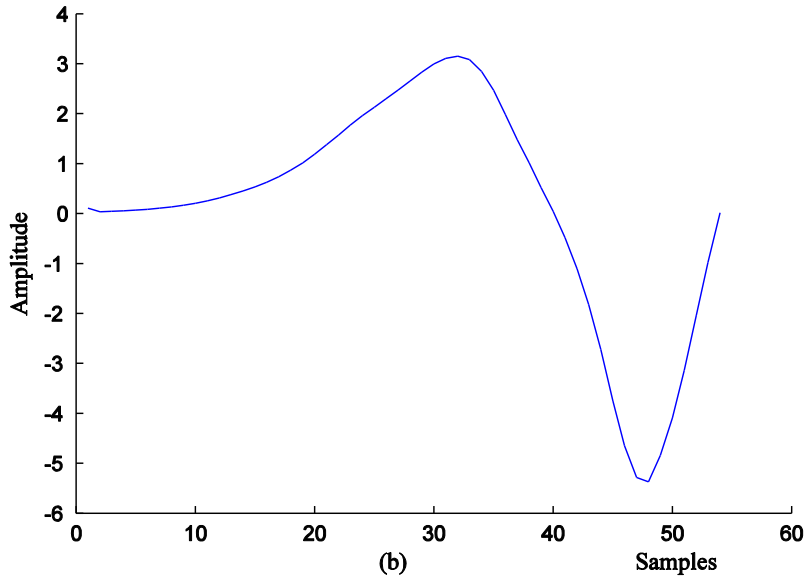

Figure 5.5 Estimation of glottal pulse for a real vowel /a/. (a) Normalized GFP (b) Derivative waveform

Figure 5.5 shows the estimation of an individual GFP and its derivative waveform for a real vowel /a/ from a male speaker after 13th-order LP analysis and phase decomposition. We notice the smooth curve occurring at the tail of the return phase of the glottal flow pulses in (a).. In Figure 5.5(b), the derivative of the signal of Figure 5.5(a) demonstrates the effects of lips radiation.

Another individual glottal flow pulse estimated for a synthetic voice sound generated by source-filter model is shown in Figure 5.6. The original glottal flow pulses were synthesized by the convolution of two exponential sequences [39] which guarantees the generated individual glottal flow pulses are of maximum-phase. Six pairs of complex conjugate poles were used to represent the vocal-tract response. Based on Figure 5.6(a) there is no curve present in the tail of the return phase. Note that a time shift occurs in

Figure 5.6(b), and there are some subtle distortions present in the open phase compared with Figure 5.6(a).

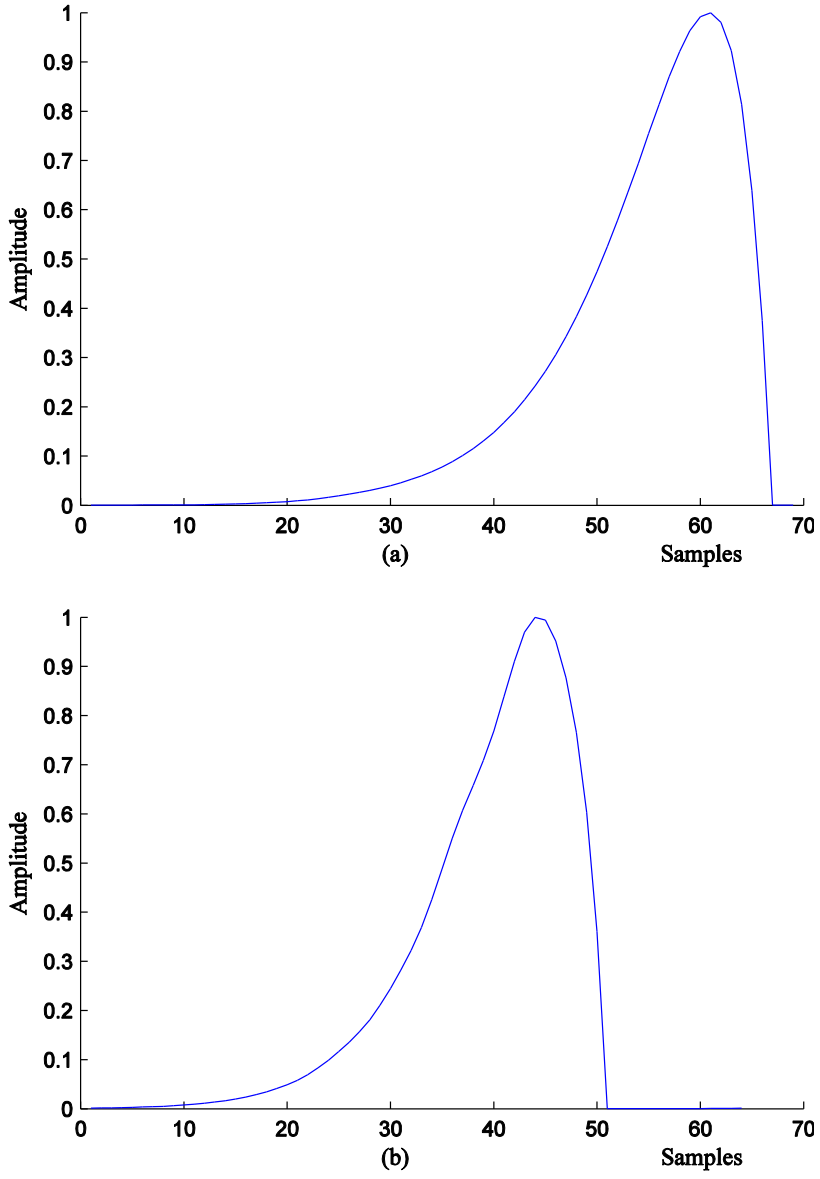

Figure 5.6 Comparison between (a) Original pulse and (b) Estimated pulse

Though the above comparison in Figure 5.6(a) and Figure 5.6(b) is direct, it is still an intuitive evaluation of our approach based on checking the difference between waveforms.

Simulations of Data Fitting

We can formulate a nonlinear least-square problem to evaluate the performance of the extraction approach by following steps:

Use LF pulses determined by a fixed parameter sets to produce excitation pulses. Then apply the excitation pulses to artificial vocal-tract response modeled by several pairs of complex conjugate poles to generate a speech signal. Next, employ the estimation approach to recover the original glottal derivative pulse used. Comparing the nonlinear LS fitting result of estimation with the original synthetic

LF derivative pulses, we can make the evaluation more quantitatively than before. Let $\hat{\mathrm{g}}[n]$ be the discrete form of derivative pulse (see equation (3.3)) fitting the estimated pulse [39] by our approach. Then we can formulate an objective value $\mathcal{E}$ which is defined by

$$\begin{aligned}\mathcal{E} &= \|\mathbf{g} - \hat{\mathbf{g}}\|^2 \\ &= \sum_i |\mathrm{g}[i] - \hat{\mathrm{g}}[i]|^2 \\ &= \sum_{i \notin [N_o, N_c]} \mathrm{g}^2[i] + \sum_{i=N_o}^{N_e-1} \left\{\mathrm{g}[i] - E_0 e^{\alpha(i-N_o)} \sin[\omega_o(i-N_o)]\right\}^2 \\ &\quad + \sum_{i=N_e}^{N_c} \left\{\mathrm{g}[i] - E_1\left[e^{-\beta(i-N_e)} - e^{-\beta(N_c-N_e)}\right]\right\}^2\end{aligned}$$

(5.10)

where N_c, N_e and N_o are discrete correspondances of T_c, T_e and T_o;

$$E_1 = E_e/1 - exp[-\beta(T_c - T_e)]$$

and

$$E_0 = E_e/exp[\alpha(T_e - T_o)]\, sin[\omega_o(T_e - T_o)].$$

So the objective function is formulated as

$$\min_{T_o,T_e,T_c,\alpha,\beta,E,\omega_o} \mathcal{E}\,.$$

There are many potential algorithms to solve this nonlinear programming LS problem [40] - [47]. However, some standard optimization methods, like Gauss–Newton with convenient and effective approximations for the Hessians, are not good candidates for a large $\mathcal{E}$ that might give rise to a rank-deficient Jacobian matrix occurring in iterations for the current piecewise data-fitting problem [11], [48]. This sort of weakness can be overcome by the introduction of a trust-region strategy.

The Levenberg-Marquardt method [49] - [51] or other Trust-Region methods [52] -[60] using the trust-region framework work well concerning this optimization case, especially the Interior-Point Trust-Region version, which were used in our experiments about nonlinear fitting. They can be regarded as an improvement on the limited memory quasi-Newton [52] method within trust regions.

The Interior-Point Trust-Region approach defines a region, normally represented by ℓ^p distance from the current reference point. The next stage of iteration is constrained to be within this region to present an overly long step from the current reference point. An objective function modeled within this region chooses the direction and size

simultaneously for the next step. If the next potential step is not successful, the method will adaptively reduce the size of current region and formulate the next minimizer. On the other hand, if the potential step is successful, the size of the current region will be enlarged. The size of the trust region is central to each step. The objective function value won't move much closer to the minimum point in the next step if the region is too small; otherwise, the objective function value of the model will be far from the minimum point of the objective function. Thus, the previous iteration's performance will uniquely determine the size of the region. A successful step explained below indicates that the current model is good over the current region and its size can be increased. A failed step indicates that the current modeling of the objective function is an inadequate expression of the objective function, and then the step size will be decreased.

A trust-region method will yield longer steps and a larger reduction in the function to be minimized, towards its potential minimum point in its trust region, than line search methods. With the iterations and adjustments of the trust region included in the optimization procedure, the algorithm converges to the local extreme value in the trust region.

For a nonlinear objective function

$$\min_{\mathbf{x}}\{f(\mathbf{x}) : \boldsymbol{\ell} \leq \mathbf{x} \leq \boldsymbol{u}\} \tag{5.11}$$

$f: \mathbb{R}^n \longrightarrow \mathbb{R}$ is the objective function with lower and upper bounds interior with a feasible set $\mathcal{F} = \{\mathbf{x} : \mathbf{x} \in \boldsymbol{\ell} < \mathbf{x} < \boldsymbol{u}\}$ where $\mathcal{F}$ is an interior box-bounded region. Thus, the scaled feasible point $\hat{\mathbf{x}}_k$ maintains the equivalent unit distance to all nearest bounds in the region $\mathcal{F}$. Distance e can be determined using

$$e = \hat{\mathbf{x}}_k - \mathcal{D}_k^{\text{affine}} \min(\mathbf{x}_k - \boldsymbol{\ell}, \boldsymbol{u} - \mathbf{x}_k) \tag{5.12}$$

where

$$\mathcal{D}_k^{\text{affine}} = \text{diag}[\min(\mathbf{x}_k - \boldsymbol{\ell}, \boldsymbol{u} - \mathbf{x}_k)]^{-1} .$$

More flexibility is provided for reducing the value of the objective function [61] - [65].

By Taylor's theorem associated with the objective function f at a value $\mathbf{q}_k$, we have the expression

$$f(\mathbf{x}_k + \mathbf{q}_k) = f(\mathbf{x}_k) + \left[\frac{\partial f(\mathbf{x}_k)}{\partial \mathbf{x}_k}\right]^T \mathbf{q}_k + \frac{1}{2}\mathbf{q}_k^T \left[\frac{\partial^2 f(\mathbf{x}_k + t\mathbf{q}_k)}{\partial \mathbf{x}_k^2}\right] \mathbf{q}_k$$

where $1 > t > 0$ and the term $R_2(\mathbf{x}_k + \mathbf{q}_k) = \frac{1}{2}\mathbf{q}_k^T \left[\frac{\partial^2 f(\mathbf{x}_k + t\mathbf{q}_k)}{\partial \mathbf{x}_k^2}\right] \mathbf{q}_k$ is the mean-value form of remainder. Then we are seeking the solution to the subproblem below for the kth step

$$\min_{\mathbf{q}_k \in \mathbb{R}^n} \left\{ f(\mathbf{x}_k) + \left[\frac{\partial f(\mathbf{x}_k)}{\partial \mathbf{x}_k}\right]^T \mathbf{q}_k + \frac{1}{2}\mathbf{q}_k^T \left[\frac{\partial^2 f(\mathbf{x}_k)}{\partial \mathbf{x}_k^2}\right] \mathbf{q}_k : \left\|\overline{\mathcal{D}}_k \mathbf{q}_k\right\| \leq \Delta_k \right\} \tag{5.13}$$

where $\mathbf{q}_k = \mathbf{x}_{k+1} - \mathbf{x}_k$ within a sufficiently small neighborhood of elliptical trust region $\left\|\overline{\mathcal{D}}_k \mathbf{q}_k\right\| \leq \Delta_k$ centered at $\mathbf{x}_k$ for current variable $\mathbf{x}_k$; $\overline{\mathcal{D}}_k$ is a scaling matrix and Δ_k is the size of trust region.

Combining both lower and upper bounds of $\mathbf{x}$, a new function $\boldsymbol{v} : \mathbb{R}^n \longrightarrow \mathbb{R}^n$ can be defined by

$$\boldsymbol{v}(\mathbf{x})^{(i)} = \begin{cases} \mathbf{x}^{(i)} - \boldsymbol{u}^{(i)}, & \text{if } \dfrac{\partial f(\mathbf{x}_k)}{\partial \mathbf{x}^{(i)}} < 0 \text{ and } \mathbf{u}^{(i)} < \infty \\ \mathbf{x}^{(i)} - \boldsymbol{\ell}^{(i)}, & \text{if } \dfrac{\partial f(\mathbf{x}_k)}{\partial \mathbf{x}^{(i)}} \geq 0 \text{ and } \boldsymbol{\ell}^{(i)} > -\infty \\ -1, & \text{if } \dfrac{\partial f(\mathbf{x}_k)}{\partial \mathbf{x}^{(i)}} < 0 \text{ and } \mathbf{u}^{(i)} = \infty \\ 1, & \text{if } \dfrac{\partial f(\mathbf{x}_k)}{\partial \mathbf{x}^{(i)}} \geq 0 \text{ and } \boldsymbol{\ell}^{(i)} = -\infty \,. \end{cases} \tag{5.14}$$

Let $\mathcal{D}_k$ be a diagonal matrix for affine scaling such that

$$\mathcal{D}_k \triangleq \text{diag}\left(1/\sqrt{|v(\mathbf{x}_k)|}\right) \,. \tag{5.15}$$

Then

$$\mathcal{D}_k^{-2} \frac{\partial f(\mathbf{x}_k)}{\partial \mathbf{x}_k} = 0$$

will be the solution to the above subproblem if the trust region size Δ_k is sufficiently large in the interior neighborhood $\mathcal{F}$ of a local minimizer. By the affine transformation, we have

$$\hat{\mathbf{x}} = \mathcal{D}_k \mathbf{x},$$

$$\hat{g}_k = \mathcal{D}_k^{-1} g_k^T = \text{diag}(|v(\mathbf{x}_k)|^{\frac{1}{2}})$$

and

$$\widehat{M} = \mathcal{D}_k^{-1}(\mathcal{B}_k + \mathcal{C}_k)\mathcal{D}_k^{-1} + \text{diag}(g_k)\mathcal{J}_k^v$$

where $\mathcal{J}_k^v$ is the Jacobian for $|v(\mathbf{x}_k)|$, $\mathcal{B}_k$ is an approximation for $\frac{\partial^2 f(\mathbf{x}_k)}{\partial \mathbf{x}_k^2}$ and

$$\mathcal{C}_k = \mathcal{D}_k \text{diag}(g_k)\mathcal{J}_k^v \mathcal{D}_k$$

where $\mathcal{C}_k$ is a positive semi-definite diagonal matrix that contains the information of constraints.

The nonlinear function

$$f(\mathbf{x}_{k+1}) = f(\mathbf{x}_k + \mathbf{q}_k)$$

can be approximated by the quadratic $\varphi(\mathbf{q}_k)$ using the Taylor Theorem. Let $\mathbf{q}_k = \mathcal{D}_k^{-1}\widehat{\mathbf{q}}_k$; then

$$\min_{\mathbf{q}_k}\left\{\varphi_k(\mathbf{q}_k) = f(\mathbf{x}_k) + g_k^T\mathbf{q}_k + \frac{1}{2}\mathbf{q}_k^T\left(\frac{\partial^2 f(\mathbf{x}_k)}{\partial \mathbf{x}_k^2} + \mathcal{C}_k\right)\mathbf{q}_k : \|\mathcal{D}_k\mathbf{q}_k\| \leq \Delta_k\right\} \qquad (5.16)$$

where

$$g_k = \frac{\partial f(\mathbf{x}_k)}{\partial \mathbf{x}_k}$$

In the neighborhood of a local minimum value, the Newton step [66] used to solve $\mathcal{D}_k^{-2}\frac{\partial f(\mathbf{x}_k)}{\partial \mathbf{x}_k} = 0$ is in fact a solution to the above trust-region problem if Δ_k is sufficiently large.

Then the trust region $\mathcal{F}$ is computed for use in the kth step or iteration. Since $\varphi_k(\mathbf{q}_k)$ is an approximation to $f(\mathbf{x}_k + \mathbf{q}_k) - f(\mathbf{x}_k) + \frac{1}{2}\mathbf{q}_k^T\mathcal{C}_k\mathbf{q}_k$, the size of trust region Δ_k would be updated by a rule based on a degree of approximation that can be measured by the ratio between actual reduction of f and predictive reduction of f:

$$\rho_k = \frac{f(\mathbf{x}_k) - f(\mathbf{x}_k + \mathbf{q}_k) + \frac{1}{2}\mathbf{q}_k^T\mathcal{C}_k\mathbf{q}_k}{\varphi_k(\mathbf{0}) - \varphi_k(\mathbf{q}_k)}. \qquad (5.17)$$

If $\rho_k \geq \mu$ which is a predefined threshold between 0 and 1, the current trust region will be enlarged by adjusting Δ_k to indicate that the objective function was reduced successfully at the kth step. If $\rho_k < \mu$, then the trust region would be compacted to imply

that the objective function was not reduced successfully at the kth step. The overall procedure can be summarized in [53] as below:

Initialization: Find a point $\mathbf{x}_0 \in \mathcal{F}$ for $1 > \mu > 0$

For $k = 1,2,\cdots$

1. Find $f(\mathbf{x}_k)$, g_k, $\mathcal{B}_k$, and $\mathcal{C}_k$.
2. Compute $\mathbf{q}_k$ as an approximate solution based on the quadratic model

$$f(\mathbf{x}_k) + g_k^T \mathbf{q}_k + \frac{1}{2}\mathbf{q}_k^T(\mathcal{B}_k + \mathcal{C}_k)\mathbf{q}_k$$

   to ensure $\mathbf{x}_k + \mathbf{q}_k \in \mathcal{F}$.
3. Compute ρ_k.
4. If $\rho_k \geq \mu$, then set $\mathbf{x}_{k+1} = \mathbf{x}_k + \mathbf{q}_k$. Otherwise, let $\mathbf{x}_{k+1} = \mathbf{x}_k$.
5. Update $\mathcal{D}_k$ and Δ_k.
6. Repeat, stating at stage 1.

The convergence analysis of the above algorithm is shown in [53].

For an arbitrary single pulse estimated by different approaches ranging from LP+CC, IAIF to ZZT to be fitted by Trust-Region methods, the pulse will be aligned with the location - T_e of the maximum negative value of the glottal pulse in Figure 5.7(a) and normalized by dividing the value of the flow derivative at T_e - E_e. Then the fitting operation is applied to the normalized version of the estimated waveform with T_e fixed. To minimize the ℓ^2 error, the shifted and normalized version is nonlinearly fitted by fixing the location of T_e and normalizing the amplitude of E_e at T_e according to the procedure summarized above. Furthermore, the estimated and fitted waveforms spanning

an interval of one pitch period will be parameterized quantitatively if the data fitting process converges successfully [67] - [73] by the above nonlinear least-square optimizer with or without constraint about net gain of the overall fitting pulse shape. By comparing the predetermined parameter set for generating the LF excitation pulse and the parameter values resulting in the fitting pulses, we can evaluate the estimation performance with a variety of approaches listed before. The parameters associated with different methods are summarized in Table 5.1.

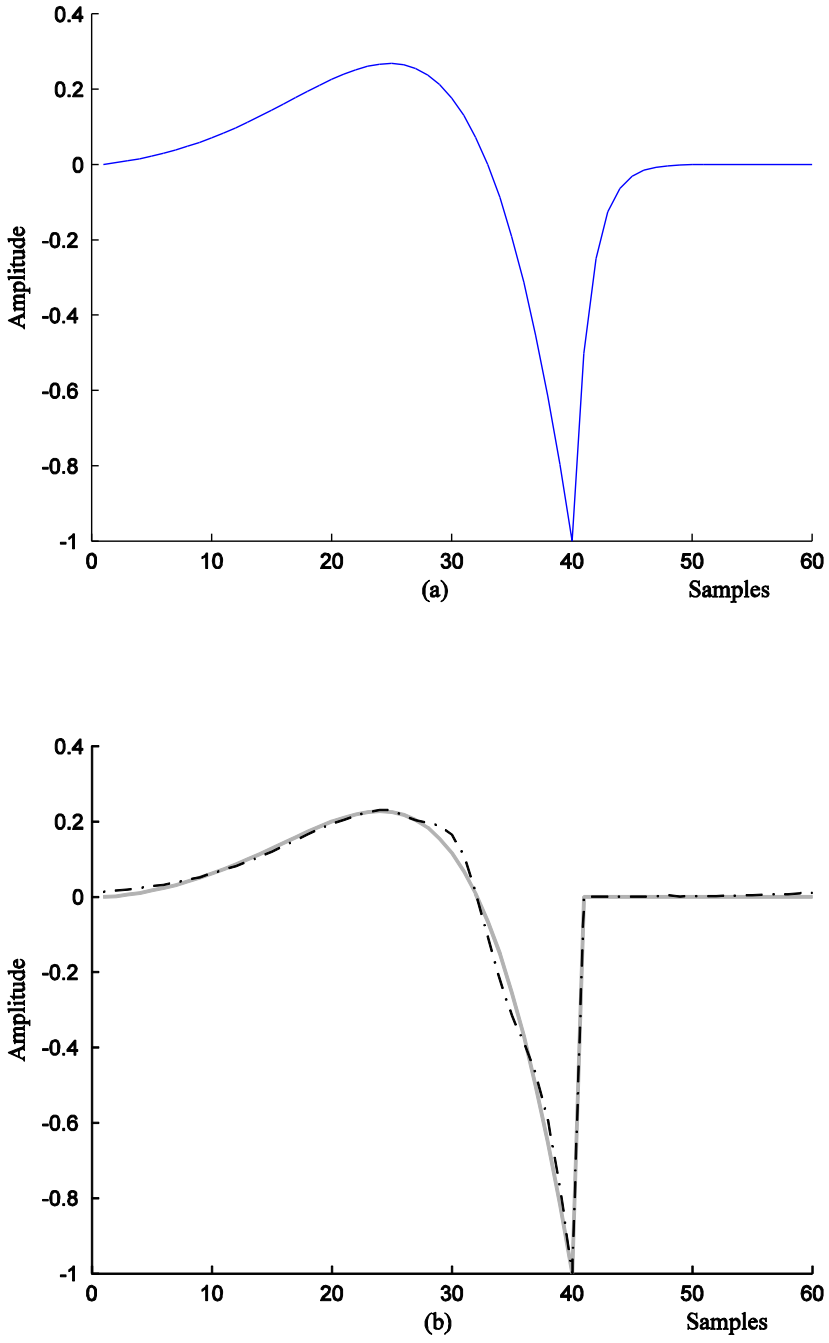

Figure 5.7 (a) Synthetic LF excitation pulse (b) Estimated pulse (black dash line) by LP+CC method

A variety of LF model based synthetic pulses containing a pulse like that shown in Figure 5.7 (a) were cascaded as the excitation to an artificial vocal-tract all-pole model with 12 complex conjugate poles to represent its coefficients. Thus, a synthetic speech utterance was generated.

The waveform estimated by the LP+CC approach in this chapter is shown in Figure 5.7(b). The open-phase portion of the waveform represented by solid gray line in Figure 5.7(b) matches well with the original synthetic pulse well; however, the returning phase expressed by a sudden discontinuity doesn't appear like the waveform in Figure 5.7 (a) because of the mix-phase characteristics of an LF model in its return-phase portion. It indicates that the LP+CC approach can deal with the pure phase components of an excitation signal of a speech utterance better than mix-phase components. Also the open-phase part of the response in Figure 5.7(b) is close to that in Figure 5.7(a).

A similar phenomenon is present for the estimation and fitting results shown in Figure 5.8 for a single pulse by the IAIF method consisting of several Linear Prediction analysis and inverse filters according to the fitting rule mentioned above. The return phase of the estimated pulse shows the discontinuity exhibited in Figure 5.7(b). Meanwhile, the ℓ^2optimization operation based on trust-region provides a fairly good LF-fitting performance over the open-phase portion for the estimated waveform represented by the black dash-dot line with amplitude distortions which were largely suppressed by LP+CC estimation in Figure 5.7(a). However, the peak of open-phase portion is higher than the original excitation pulse.

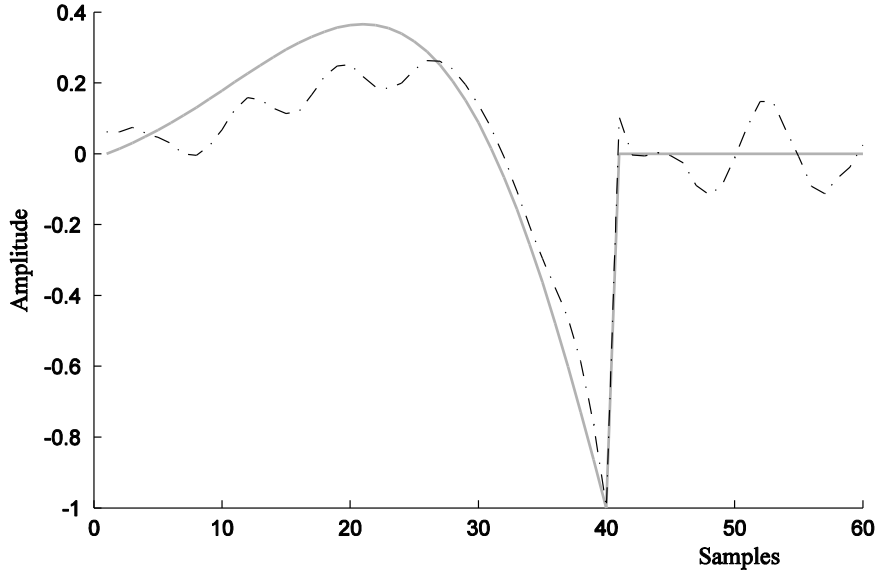

Figure 5. 8 Estimated pulse (black dash line) by IAIF method

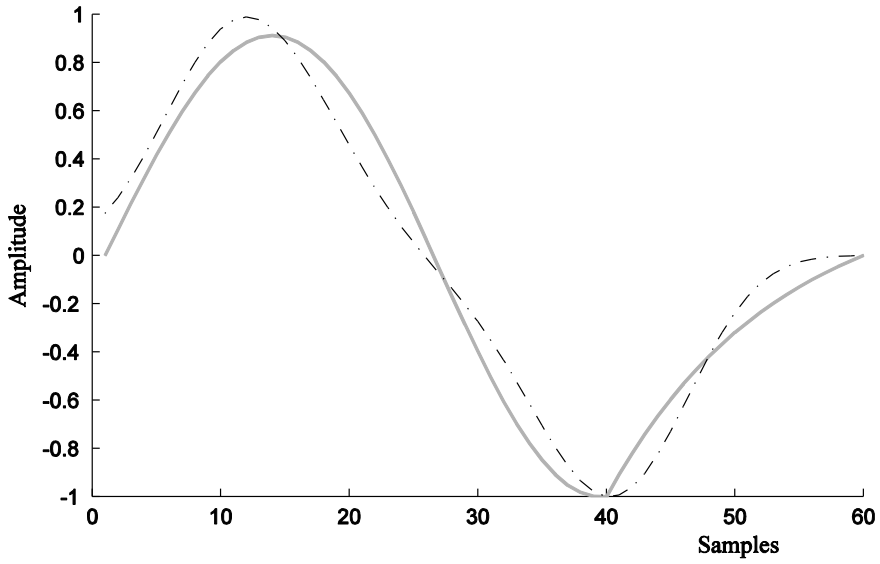

Figure 5. 9 Estimated pulse (black dash line) by ZZT method

The ZZT method that separates maximum-phase from minimum-phase of speech signal has an inferior estimation and resulting fitting results in Figure 5.9 comparing with its counterpart in Figure 5.7(b) and Figure 5.8.

Although methods like LP+CC and IAIF have noticeable distortion when used to recover the information contained in the close-phase region of LF model, they still recover valuable information inside the open-phase region. All LF shaping parameters and their quantities associated with these three distinct excitation estimation methods are listed in Table 5.2 with their sample estimated pulses truncated by the window with length of the synthetic pulse positioned at T_e.

	T_o	t_p	α	β	ℓ^2 error/ Energy (Percent)
Synthetic Pulse	1	32	0.095	0.69	N/A
Fitting Pulse (LP+CC)	1.881	30.22	0.094	15.451	12.18%
Fitting Pulse (IAIF)	1.004	30.197	0.058	12.4346	16.64%
Fitting Pulse (ZZT)	1	25.55	0.0037	0.0756	63.21%

Table 5.1 Comparison of parameters of synthetic and fitting excitation pulses from different methods

Based on the quantities summarized in Table 5.1, we conclude that the two estimation methods involving LP analysis and inverse filtering (LP+CC and IAIF) have an advantage over the ZZT method. The separation of vocal-tract and GFP information based on phase separation can be used to improve the result. But this approach lacks

some accuracy while dealing with the LF synthetic model in this set of experiments. The fidelity of the open-phase portion of the original excitation information can be largely preserved by LP analysis and its inverse filtering. Thus, it becomes at least a practical benefit to extract real speakers' excitation pulses for vowels and voiced sounds as their private physical features as described in chapter 7.

Summary

In this chapter, we presented an improved approach based on the jointly parametric and nonparametric estimation for vowels. Unlike most existing conventional LP applications, we formulated an odd-order all-pole model to cancel the formants from the vocal-tract response by inverse filtering, the result of which gives a way for further refinement in terms of GFPs because of the obtaining of rough pulses after LP analysis and inverse filtering. The phase characteristics of GFP and vocal-tract responses enable us to employ the CC as a phase-decomposition based method to split the maximum-phase and minimum-phase components of the signal from each another. Thus, this gives us an effective way to enhance the estimation results from LP analysis.

As we employ limited data for each shifted LP window and apply inverse filtering to estimate individual glottal pulses represented by open, return and close phase, we can easily cascade these estimated pulses together to form a train together with the information of pitch length variation. Therefore, the estimation results can be further developed synchronously to recover a pulse train. The high computation-cost closely associated with the detection of GCIs to locate an adequate pitch for analysis in phase-

decomposition methods can be avoided. According to what we have achieved in this chapter, we can evaluate the effectiveness of the proposed method for extracting features of real speech for a number of speech processing applications. An example of these applications will be introduced in chapter 7 as another approach to evaluate our method.

CHAPTER SIX

JOINTLY PARAMETRIC AND NONPARMETRIC ESTIMATION METHODS OF GLOTTAL FLOW PULSES II

Covariance methods of LP analysis typically based on all-pole models representing the human vocal tract once dominated the glottal pulse extraction task [17], [18]. They adapt LS algorithms to find the parameters for their models given the model type and the number of parameters. Model-based approaches must assume model types and model orders as a priori information; however, a priori information is generally unknown. Thus, there are always some inaccuracies in these model-base approaches.

As a single LF model [7] was found by polynomial analysis to have the glottal pulse return phase being mixed-phase [10]. Some nonparametric methods [31], [32] have been used for the decomposition between the maximum-phase and minimum-phase parts of speech signals. The decomposition results proved helpful to perform the source-tract separation. Also the introduction of LS residual errors as a result of LP analysis affects the extraction. Both of these two concerns will be taken into accounts while we design a further processing procedure.

Higher-order homomorphic filtering is able to deal with the phase decomposition and the suppression of noise introduced by the LP analysis and its corresponding inverse filtering upon the speech sequence. The bicepstrum expression can be used to separate the maximum and minimum-phase components [74]. The cumulant and cepstrum are based on higher-order statistical (HOS) methods which help suppress effects of additive noise and whitening residual errors which are byproducts of inverse filtering by coefficients of LP analysis.

We here design an odd-order all-pole predictor to implement the LP analysis. If the vocal-tract is lossy, it is assumed to be minimum-phase and represented by inside-unit-circle complex conjugate poles of an all-pole model. Therefore, any individual glottal pulse will be represented by at least one real pole from the model. First, we can get a rough representation after the inverse filtering was applied to the original observed speech sequence. Then we can improve the inverse-filtering results by applying HOS processing to perform phase decomposition. And the bicepstrum representation of coarse pulses will largely help suppress the errors coming from LS estimation in LP covariance analysis.

Brief Background on Higher-Order Statistics

The covariance method of LP analysis together with an optimization algorithm results in lower residual error level than the autocorrelation method which is based on second-order statistics. Also, the autocorrelation function used in the autocorrelation method will eliminate all phase information. Fortunately, we can look beyond second-order statistics with help of higher-order cumulants given by [75]

$$R_X^{(n)} = \frac{d^n \ln \Phi_X(s)}{ds^n}, \qquad n > 2$$

where $\Phi_X(s) = \mathbb{E}[e^{sX}]$ is the moment generating function of random variable X.

If the order of statistical analysis is increased enough to look beyond the domain of correlation and its frequency counterpart, we are able to find the magnitude and phase information without the assumption about models, the number of model parameters, and linearities of the system. The third-order cumulants, bispectrum and bicepstrum have

been widely applied in signal reconstruction and detection because of their less computation costs compared with fourth and higher order statistics approaches. The third-order cumulant for a stationary process X_n is denoted by

$$R_X^{(3)}(k_1,k_2) = m_X^{(3)}(k_1,k_2) - m_X^{(1)}\left[m_X^{(2)}(k_1) + m_X^{(2)}(k_2) + m_X^{(2)}(k_1-k_2)\right] + 2\left(m_X^{(1)}\right)^3 \tag{6.1}$$

where

$$m_X^{(3)}(k_1,k_2) = \mathbb{E}[X(k)X(k+k_1)X(k+k_2)]$$

and

$$m_X^{(2)}(k_1) = \mathbb{E}[X(k)X(k+k_1)]$$

and

$$m_X^{(1)} = \mathbb{E}[X(k)]$$

Thus, $m_X^{(1)}$, $m_X^{(2)}(\cdot)$ and $m_X^{(3)}(\cdot,\cdot)$ are respectively first, second and third order statistical average operators. $R_X^{(3)}(k_1,k_2)$ can be obtained by averaging observed data [76] - [84].

Now we are concentrating on the bicepstrum to conduct phase separation as we did for the complex cepstrum. We will evaluate the potential improvement compared with existing methods.

The bicepstrum is given by

$$\hat{\mathrm{c}}_X^{(3)}(\tau_1,\tau_2) = \mathcal{F}^{-2}\left\{\ln \mathcal{F}^2\left[R_X^{(3)}(k_1,k_2)\right]\right\} \tag{6.2}$$

The estimated bispectrum of the sum of two sinusoidal signals is shown in Figure 6.1.

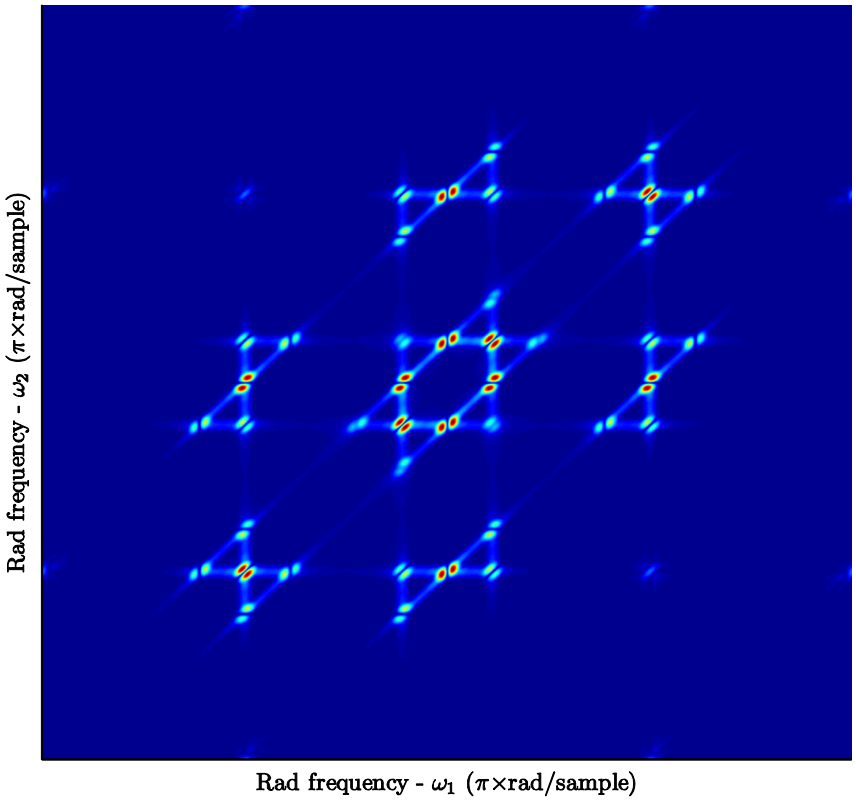

Figure 6.1 Illustration of bispectrum of $\sin\frac{\pi}{2}n + \sin\frac{\pi}{9}n$

Odd-Order Linear Prediction

Consider a speech signal X_n, for which the $\mathcal{Z}$-transform is denoted by

$$X(z) = G(z)H(z)\,. \tag{6.3}$$

Equation (6.3) represents the response of GFPs and the lip radiation modeled by the first-order difference equation, and $H(z)$ is the response of vocal tract that is a minimum-phase system [25], which might contain zeros. $H(z)$ can be represented by

$$H(z) = H_{az}(z)H_{ap}(z)$$

$$= H_{az}(z)H_{ap\_real}(z)H_{ap\_comp}(z)$$

where $H_{az}(z)$ denotes all-zero part and $H_{ap}(z)$ denotes all-pole part of vocal-tract response. The estimate of $G(z)$ and $H(z)$ leads to the source-tract separation.

Covariance methods of LP analysis, usually with even order, have become a major tool for the parametric analysis of voiced speech utterances [17], [18] since they can represent resonance frequencies characterizing the speaker's vocal tract. On the other hand, an odd-order all-pole model expressed by

$$\widehat{H}_{ap}(z) = \frac{1}{1 - \sum_{m=1}^{2M+1} a_m z^{-m}}$$

guarantees that at least one real pole represents the low-pass tilting effect of the glottal source. Then we can separate $\widehat{H}_{ap}(z)$ into two systems $\widehat{H}_{ap\_comp}(z)$ contributed by complex pole pairs and $\widehat{H}_{ap\_real}(z)$ contributed by real poles.

$$X(z) = \widehat{H}_{ap}(z)\Xi(z) \tag{6.4}$$

holds after inverse filtering with $\widehat{H}_{ap}(z)$ obtained from LP analysis applied to $X(z)$. Here $\boldsymbol{\xi}_n \overset{\mathcal{Z}}{\longleftrightarrow} \Xi(z)$ and $\boldsymbol{\xi}_n$ denotes the vector of LP residual errors.

Let $\mathbf{x}_n = \left[x_1^{(n)}, \ldots, x_N^{(n)}\right]^T \in \mathbb{R}^N$ be a windowed discrete-time speech frame and $\hat{\mathbf{x}}_n = \widetilde{\mathbf{X}}_n \mathbf{a}_n$ be the optimum estimate of $\mathbf{x}_n$ in LS sense, then the all-pole model coefficients vector $\mathbf{a}_n = \left[a_1^{(n)}, \cdots, a_{2M+1}^{(n)}\right]^T$ is found to minimize the ℓ^2 norm error between the observed signal $\mathbf{x}_n$ and its estimation $\hat{\mathbf{x}}_n$. In general,

$$\underset{\mathbf{a}_n}{\operatorname{argmin}} \left\| \mathbf{x}_n - \widetilde{\mathbf{X}}_n \mathbf{a}_n \right\|$$

where $\widetilde{\mathbf{X}}_n \in \mathbb{R}^{N\times(2M+1)}$ is a data matrix shown in (5.3) and $\hat{\mathbf{a}}_n$ can be determined by recursive LS algorithms.

Given a predictor coefficient vector $\hat{\mathbf{a}}_n$ with an odd number of elements, there exists at least one real root $p_i \in \mathbb{R}$, such that

$$\cdots(1-p_i z^{-1})\cdots = 1-\sum_{m=1}^{2M+1}\hat{a}_m z^{-m}$$

as the result of LS estimation. Then the remaining complex poles from $\mathcal{P}$ excluding p_i are reserved for the representation of the coarse vocal-tract response, here $\mathcal{P}$ is the set of all roots of the above polynomial.

These estimated complex conjugate poles form a linear filter to deconvolve the observed speech signal to obtain the coarse representation of the glottal source corresponding to the current windowed speech frame. This leads to the estimated glottal excitation $\mathbf{e}[n] \overset{\mathcal{Z}}{\longleftrightarrow} E(z)$ expressed by

$$E(z) = \frac{X(z)}{\widehat{H}_{ap\_comp}(z)} = \widehat{H}_{ap\_real}(z)\Xi(z) \tag{6.5}$$

where $\widehat{H}_{ap\_real}(z)$, the estimation of $H_{ap\_real}(z)$, might contain some components from the resonances $H_{ap\_comp}(z)$ of the speaker's vocal tract.

In next step, we need to refine the glottal source estimates by removing those remaining components of the vocal-tract response after the LP analysis and inverse filtering. Meanwhile, how to suppress LS residual errors $\Xi(z)$ and the additive noise is another concern in our approach.

High-Order Homomorphic Filtering

Rough results from the odd-order LP analysis and inverse filtering form a good beginning for synchronized processing since the glottal closure instants becomes obvious. From the phase characteristics of glottal source and vocal-tract responses, the phase decomposition could be effective [31], [32] for dealing with the results from inverse filtering, in which complex conjugate poles play an important role to cancel formants in speech. HOS methods can be invoked to suppress the residual errors which are akin to white noise. Based on the bicepstrum from the third-order cumulants of the current speech sequence frame, we are able to achieve the refinement of individual glottal flow pulses.

Consider a finite-length segment $\mathbf{y}_m$ spanning slightly larger than one pitch period within the estimated glottal source in Figure 6.1, and let $R_{\mathbf{y}}^{(3)}(k_1, k_2)$ denote the third-cumulant in Figure 6.2 from an indirect estimator [85]. Notice the tilting effect due to the bias [21].

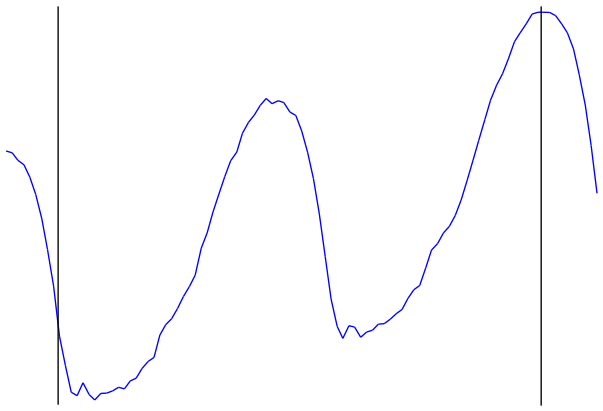

Figure 6.2 Analysis region after LP analysis

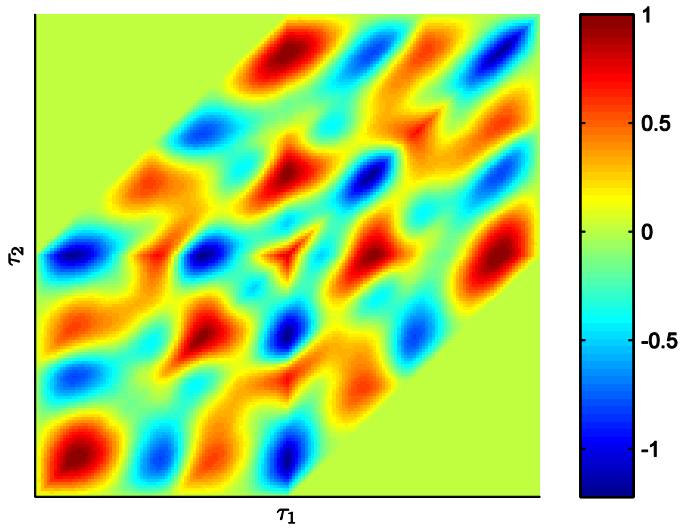

Figure 6.3 The 3rd-order cumulant of the finite-length sequence $\mathbf{y}_m$

From (6.5), a linear convolution relation holds

$$\mathbf{y}_m = \boldsymbol{\xi}_m * \widehat{\boldsymbol{h}}_m \tag{6.6}$$

where $\widehat{\boldsymbol{h}}_m$ denotes the impulse response of the estimated glottal source corresponding to the real pole or poles of $\widehat{H}_{ap\_real}(z)$ in (6.5), and $\mathbf{y}_m$ denotes estimated excitation. Applying the two-dimensional $\mathcal{Z}$-transfrom to $R_{\mathbf{y}}^{(3)}(k_1, k_2)$, we obtain

$$\mathrm{c}_{\mathbf{y}}^{(3)}(z_1, z_2) = \mathcal{Z}^2\left\{R_{\mathbf{y}}^{(3)}(k_1, k_2)\right\}$$

to suppress additive noise where $\mathrm{c}_{\mathbf{y}}^{(3)}(z_1, z_2)$ is the bispectrum of $\mathbf{y}_m$. If the residual error response $\boldsymbol{\xi}_m$ is assumed to have white noise-like properties between two successive impulses, then from Appendix A, we have the bicepstrum $\mathrm{c}_{\mathbf{y}}^{(3)}(z_1, z_2)$ corresponding to the random output of linear system $h(k)$ shown below

$$R_{\mathbf{y}}^{(3)}(\tau_1,\tau_2)=\gamma_{\boldsymbol{\xi}}^{(3)}\sum_{k=-\infty}^{\infty}h(k)h(k+\tau_1)\,h(k+\tau_2)\,. \tag{6.7}$$

Furthermore, the bispectrum is

$$\begin{aligned}\mathrm{c}_{\mathbf{y}}^{(3)}(z_1,z_2)&=\mathcal{Z}^{-2}\left\{R_{\mathbf{y}}^{(3)}(\tau_1,\tau_2)\right\}\\&=\gamma_{\boldsymbol{\xi}}^{(3)}\cdot\beta\cdot(2\pi)^{-2}H(z_1)H(z_2)H^{*}(z_1z_2)\end{aligned} \tag{6.8}$$

where $\gamma_{\boldsymbol{\xi}}^{(3)}$ is the skewness of $\boldsymbol{\xi}_m$ and β is the system gain. The system response $H(z_1)$ is given by

$$H(z_1)=A_1\mathcal{I}(z_1^{-1})\mathcal{O}(z_1)z_1^{-r_1}$$

where A_1, $\mathcal{I}(z_1^{-1})$ and $\mathcal{O}(z_1^{-1})$ respectively denote the system gain, minimum-phase and maximum-phase components of $H(z_1)$. Meanwhile, the linear phase term $z_1^{-\ell}$ could be removed by phase unwrapping. Similarly, we have

$$H(z_2)=A_2\mathcal{I}(z_2^{-1})\mathcal{O}(z_2)z_2^{-r_2}$$

and

$$H^{*}(z_1z_2)=A_{1,2}\mathcal{I}(z_1^{-1}z_2^{-1})\mathcal{O}(z_1z_2)(z_1z_2)^{r_{1,2}}\,.$$

Thus the bicepstrum $\mathrm{c}_{\mathbf{y}}^{(3)}$ of $\mathbf{y}_m$ not considering linear phase terms is given by

$$\mathrm{c}_{\mathbf{y}}^{(3)}(z_1,z_2)=\gamma_{\boldsymbol{\xi}}^{(3)}\cdot\beta\cdot\mathcal{I}(z_1^{-1})\mathcal{O}(z_1)\mathcal{I}(z_2^{-1})\mathcal{O}(z_2)\mathcal{I}(z_1^{-1}z_2^{-1})\mathcal{O}(z_1z_2) \tag{6.9}$$

where $\beta=A_1A_2A_{1,2}$ is the gain. The natural logarithm expression of $\mathrm{c}_{\mathbf{y}}^{(3)}(z_1,z_2)$ is given by

$$\ln \mathrm{c}_{\mathbf{y}}^{(3)}(z_1, z_2) = \ln\left|\gamma_{\xi}^{(3)}\beta\right| + \ln \mathcal{I}(z_1^{-1}) + \ln \mathcal{I}(z_2^{-1}) + \ln \mathcal{I}(z_1^{-1}z_2^{-1}) + \ln \mathcal{O}(z_1) + \ln \mathcal{O}(z_2) + \ln \mathcal{O}(z_1 z_2)\,. \tag{6.10}$$

The bicepstrum $\hat{\mathrm{c}}_{\mathbf{y}}^{(3)}(k_1, k_2)$ in the two-dimensional plane after taking inverse $\mathcal{Z}^{-1}$ transform of $\ln \mathrm{c}_{\mathbf{y}}^{(3)}(z_1, z_2)$ is given by [74]

$$\hat{\mathrm{c}}_{\mathbf{y}}^{(3)}(k_1, k_2) = \mathcal{Z}^{-1}\left\{\ln \mathrm{c}_{\mathbf{y}}^{(3)}(z_1, z_2)\right\} = \begin{cases} \ln\left|\gamma_{\xi}^{(3)}\beta\right|, & k_1 = 0, k_2 = 0 \\ -\dfrac{1}{k_2}A^{(k_2)}, & k_1 = 0, k_2 > 0 \\ -\dfrac{1}{k_1}A^{(k_1)}, & k_2 = 0, k_1 > 0 \\ \dfrac{1}{k_1}B^{(-k_1)}, & k_2 = 0, k_1 < 0 \\ \dfrac{1}{k_2}B^{(-k_2)}, & k_1 = 0, k_2 > 0 \\ -\dfrac{1}{k_2}B^{(k_2)}, & k_1 = k_2 > 0 \\ \dfrac{1}{k_2}A^{(-k_2)}, & k_1 = k_2 < 0 \\ 0, & \text{otherwise} \end{cases} \tag{6.11}$$

All bicepstrum quantities except those at the origin along the axis $k_1 = 0$ can be expressed as

$$\hat{\mathrm{c}}_{\mathbf{y}}^{(3)}(0, k_2) = \begin{cases} -k_2^{-1}A^{(k_2)}, & k_2 > 0 \\ k_2^{-1}B^{(-k_2)}, & k_2 < 0 \end{cases} \tag{6.12}$$

where $A^{(i)}$ and $B^{(j)}$ as differential cepstrum [85] terms are mapped to the bicepstrum plane to derive the complex cepstrum $\hat{\mathrm{c}}_{\mathbf{y}}(k_2)$ with the property [74], [87]

$$\hat{\mathrm{c}}_{\mathbf{y}}^{(3)}(0, k_2) = \hat{\mathrm{c}}_{\mathbf{y}}(k_2)\,.$$

Since maximum-phase components $\hat{\mathrm{c}}_{\mathbf{y}}^{(\ell)}(k_2)$ and minimum-phase components $\hat{\mathrm{c}}_{\mathbf{y}}^{(r)}(k_2)$ lie in the left and right hand of origin of cepstrum plane, we can recover both maximum-phase $\mathbf{i}_m$ and minimum-phase impulse response $\mathbf{o}_m$ by applying an operator $\mathcal{D}_*^{-1}[\,\cdot\,]$ to $\hat{\mathrm{c}}_{\mathbf{y}}^{(\ell)}(\tau_2)$ and $\hat{\mathrm{c}}_{\mathbf{y}}^{(r)}(\tau_2)$. Here $\mathcal{D}_*^{-1}[\,\cdot\,]$ is the reverse transform of $\mathcal{D}_*[\,\cdot\,]$ where $\mathcal{D}_*[\mathbf{r}_n] = \hat{\mathrm{c}}_{\mathbf{r}}(n)$. Then the maximum-phase component $\mathbf{i}_m$ can be reserved as a refined GFP [19].

However, we need to consider linear phase terms in (6.10) and corresponding effects from those. Note that two-dimensional phase unwrappings to overcome phase discontinuities before applying the natural logarithm to the bispectrum will be much harder than what we did to calculate the cepstrum in one-dimensional case. We can circumvent the two-dimensional phase unwrapping by utilizing the relation [74], [85]

$$R_{\mathbf{y}}^{(3)}(k_1, k_2) * \left[-k_1 \hat{\mathrm{c}}_{\mathbf{y}}^{(3)}(k_1, k_2)\right] = -k_1 R_{\mathbf{y}}^{(3)}(k_1, k_2) \tag{6.13}$$

where "$*$" denotes two-dimensional convolution operator. A set of cepstral equations derived from above expression are listed in [85] as

$$\sum_{i=1}^{p} A^{(i)}\left[R_{\mathbf{y}}^{(3)}(k_1 - i, k_2) - R_{\mathbf{y}}^{(3)}(k_1 + i, k_2 + i)\right] + \sum_{j=1}^{q} B^{(j)}\left[R_{\mathbf{y}}^{(3)}(k_1 - i, k_2 - j) - R_{\mathbf{y}}^{(3)}(k_1 + i, k_2)\right] \cong -k_1 R_{\mathbf{y}}^{(3)}(k_1, k_2) \tag{6.14}$$

where p and q are parameters to restrict the numbers of coefficients $A^{(i)}, B^{(j)}$ and $1 \le i \le p, 1 \le j \le q$.

Simulation Results

In order to evaluate the performance of the proposed approach of estimating individual GFPs, two sets of experiments were performed. A sampling rate of 8kHz was used.

An estimation of a GFP from a real vowel /a/ from a male speaker is shown in Figure 6.4. The pulse which results from the inverse filtering in Figure 6.2 behaves as an input to a conventional indirect estimator [84] for the third-order cumulant with $p = 62$ and $q = 2$ after comparing different combinations of p and q values [86], [87].

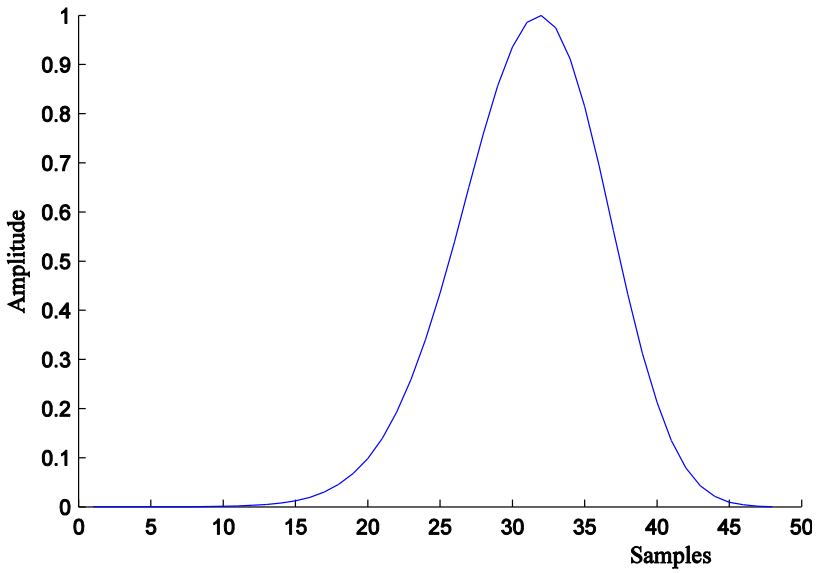

Figure 6.4 Normalized GFP estimation from a real vowel /a/

Another single pulse is generated in Figure 6.5(a) by convolution of two exponential sequences [39].

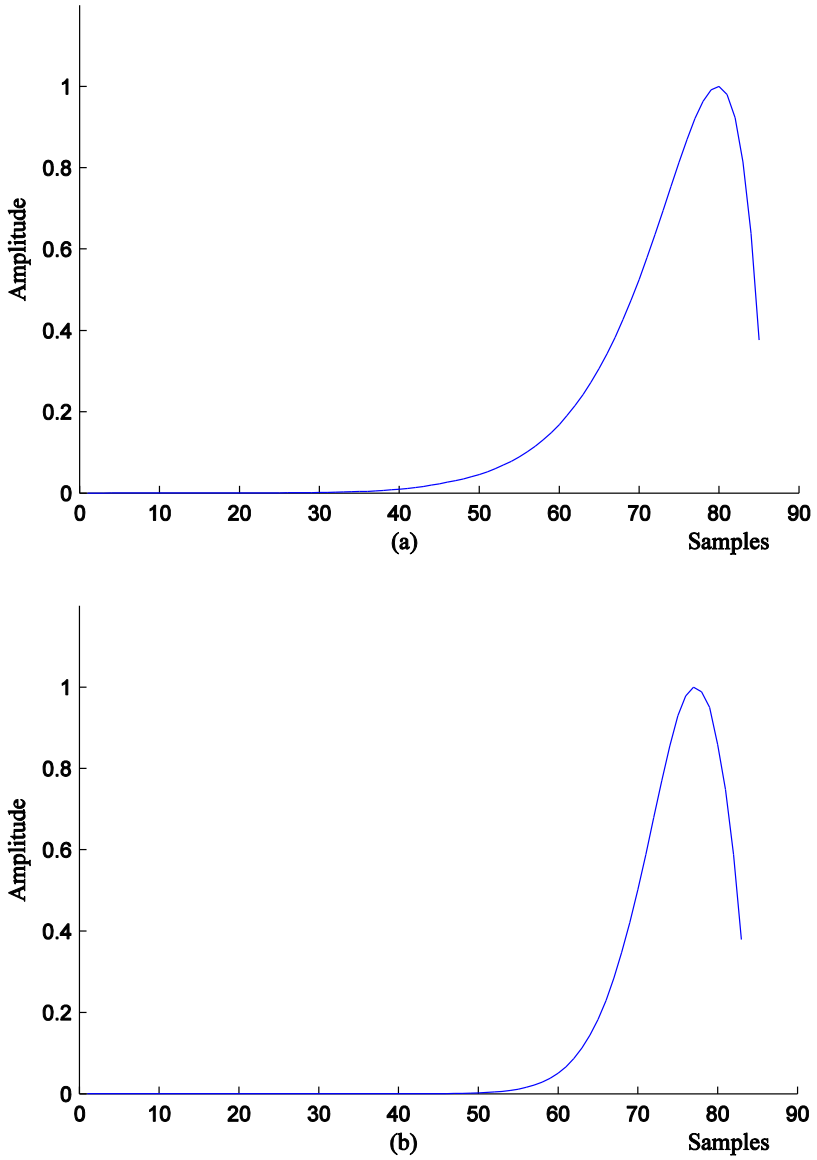

Figure 6.5 Illustration of (a) Original GFP used to generate voiced Speech sequence (b) Estimated GFP resulting from LP and bicepstrum-decomposition

Concatenating the duplications of a single pulse, we created a train of glottal excitations to the cascaded second-order resonance systems and first-order difference equations modeling of the vocal tract and lips radiation responses, respectively, while synthesizing a sustained voiced speech utterance. After applying the HOS GFP

estimation approach, we can recover the excitation signal, especially, individual pulses. The process can be summarized by Figure 6.6.

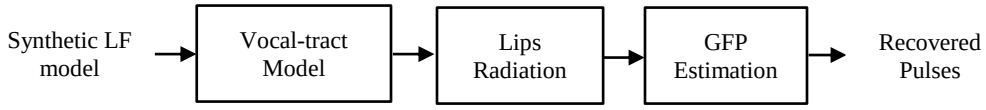

Figure 6.6 Workflow to recover exciting synthetic glottal pulse

A comparison can be made through the single pulse estimation shown in Figure 6.5(b) as the result of 12-pole inverse filtering and HOS homomorphic filtering of one segment of observed data. Notice that the estimated GFP shown in Figure 6.5(b) has a steeper decreasing attenuation than that of in Figure 6.4(a) in its open-phase portions. This distortion is normally introduced by insufficient samples while calculating the average [88]. The waveform shown in Fig. 6.5(b) is free of whitening residue errors since they were suppressed by the bicepsturm method already described. The bicepstrum quantities along the axis $k_1 = 0$ axis are obtained, while the origin is discarded.

A quantitative comparison was calculated of parameter sets between the synthetic pulse and fitted waveform to analyze the performance of the estimation methods based on our observations of data excited by cascaded synthetic LF models with those known parameters.

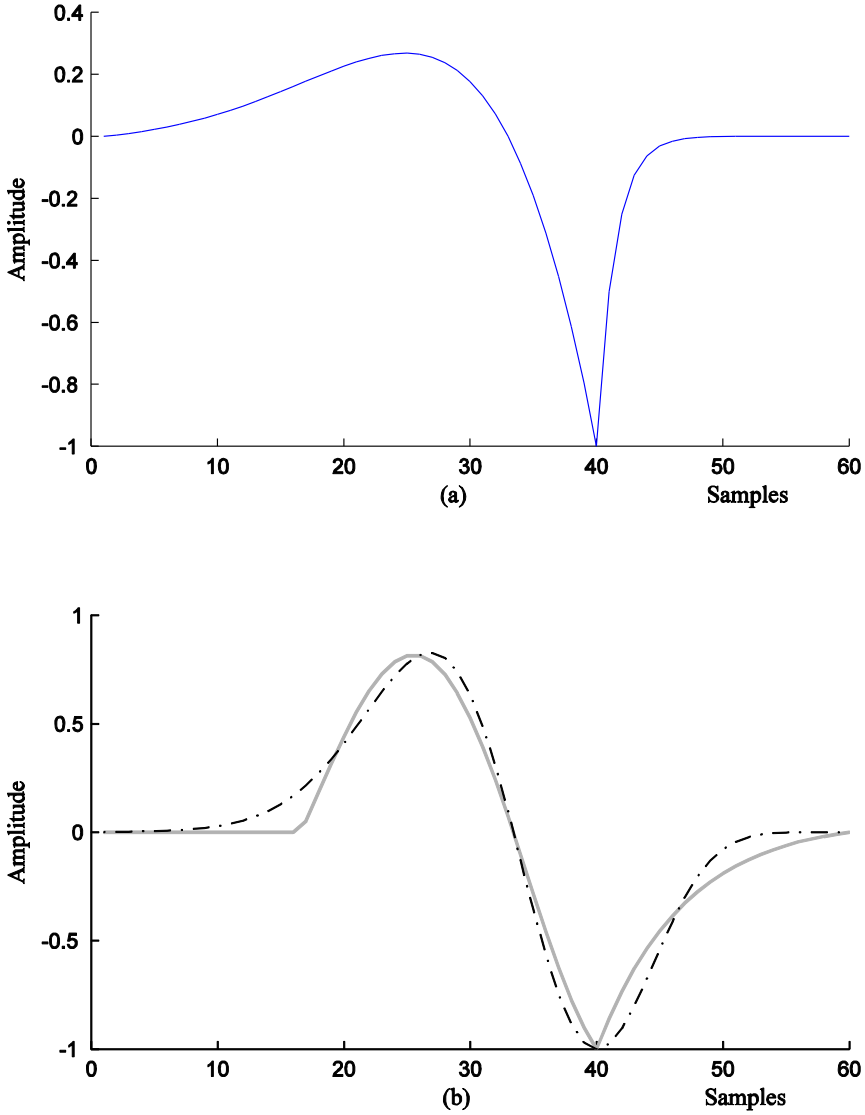

Figure 6.7 (a) Synthetic LF excitation pulse (b) Estimated pulse (black dash line) and fitted pulse (gray solid line)

	T_o	t_p	α	β	ℓ^2 error/ Energy (Percent)
Synthetic Pulse	1	32	0.095	0.69	N/A
Fitting Pulse	16.6	16.8	0.0177	0.144	35.54%

Table 6.1 Comparison of parameters of synthetic and fitted excitation pulses

The peak value of overshoot of the estimated pulse in the open phase in Figure 6.7 (b) exceeds that of the pulse shown in Figure 6.7(a). Also, the values of the parameter α, t_p and T_o for the synthetic pulse differ from those of the fitted pulses. These three parameters and β determine the shape of fitted pulse in open phase. See Table 6.1. The overall ℓ^2 fitting error implies that it has better performance than the pure phase separation method with the LF model used to represent the excitation pulse. Several papers [84], [89] mentioned that higher-order statistics are immune to Gaussian noises. The distortions shown in Figure 5.6(b) can be suppressed.

Summary

In this chapter, we presented a technique combining LP and HOS processing to estimate and model the GFP waveform for voiced speech sounds. The return-phase information can be estimated and the residue errors from LP analysis due to the inverse filtering after LP covariance analysis can be suppressed. A large computation cost of accurate GCI detections [9] can be avoided if the inverse filtering is applied to find

coarse estimation of GFPs with the reciprocal of complex conjugate poles from an all-pole LP model. However, the lack of prior information while setting parameter p and q might bring distortions to estimated pulses.

CHAPTER SEVEN

A SMALL SCALE SPEAKER IDENTIFIER WITH LIMITED EXCITING INFORMATION

As glottal pulses had been intuitively to consider containing excitation information from a specific speaker, the estimated glottal pulse in chapter 5 gives us a direct representation of the continuous information as pulses in waveform. Extracting parameter values from the continuous information to form speaker's features, we can try to apply these new feature values to training models for speaker recognition. Followed by a maximum and minimum phase separation operation, the glottal pulses are estimated using linear prediction followed by its inverse filtering by estimated LP all-pole coefficients. These estimated waveforms can be fitted by a new LF glottal flow derivative model whose shape can be adjusted through its parameters to minimize the least-square errors between target waveform and fitting model as previously described in chapter 5.

Estimating these LF model parameters obtained from the inverse filtering of linear prediction applying to the original speech, and complex cepstrum coefficients, we set up a training set for each speaker who was used as a test subject later on in the realization of a speaker identification system. Then a classification system based on minimum distance rule is applied to testing data for each subject to decide which centroid is nearest to the current testing subject among all centroids in the sense of least Minkowski-distance or by other metrics. Then labels corresponding to centroids can be assigned to all observed testing features in this way. The identifiability of speech features in terms of estimated glottal flow pulses of all subjects is thus determined as a result of the experiment.

Overall Scheme of the Speaker Identifier

What makes a speaker identification based on specific phonemes different from other speech or speaker recognition systems is the limited number of training and testing features. We had only a small amount of observed data to build models to find their statistical properties. The minimum-distance classifier, based on vector quantization, to choose nearest neighbor is employed as shown in Figure 7.1 shows in [90] - [99].

Let $\mathcal{U} = \{\mathbf{x}_1, \mathbf{x}_2, \cdots, \mathbf{x}_n\}$ be the set of all observed feature vectors and $\mathcal{O} = \{\mathbf{y}_1, \mathbf{y}_2, \cdots, \mathbf{y}_k\}$ be the set of centroids between training data where $\mathcal{U} \in \mathbb{R}^r$ is a testing feature space and $\mathcal{O} \in \mathbb{R}^r$ is a training feature space. Let $\mathcal{V} = \{\vartheta_1, \ldots, \vartheta_k\}$ be a corresponding label associated with each $\mathbf{y}_i$, $1 \leq i \leq k$, in the set $\mathcal{O}$. For a general identification problem, the task is to find a mapping $f : \mathcal{U} \to \mathcal{V}$ knowing observation space $\mathcal{U}$ and parameter space $\mathcal{V}$. According to the metric of the distance between two points $\mathbf{x} \in \mathcal{U}$ and $\boldsymbol{y}_i \in \mathcal{O}$, we can furthermore find the optimum f^* by

$$f^* = \underset{\mathbf{y}_i \in \mathcal{O}, \vartheta \in \mathcal{V}}{\operatorname{argmin}} \, m\,(\mathbf{x}, \mathbf{y}_i; f, \vartheta)$$

with measure operator $m(\cdot)$ based on the Minkowski distance $\|\mathbf{x} - \mathbf{y}\|_p$ where p is alterable depending on characteristics of these points. Different metrics are applied to the speaker identification system with different p values.

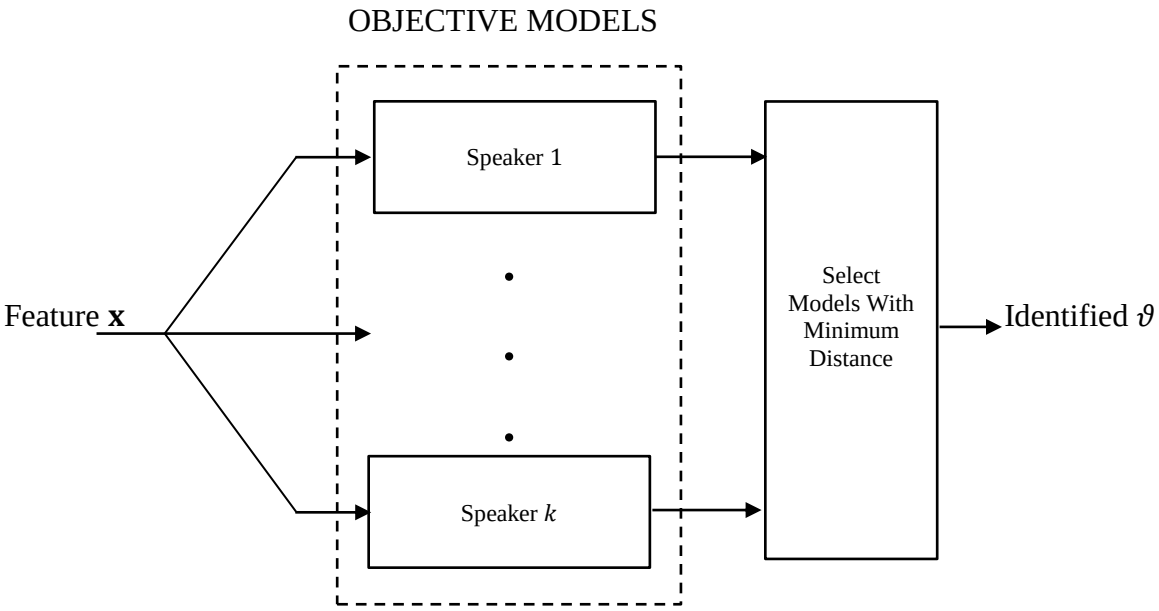

Figure 7.1 Speaker identification system to choose models

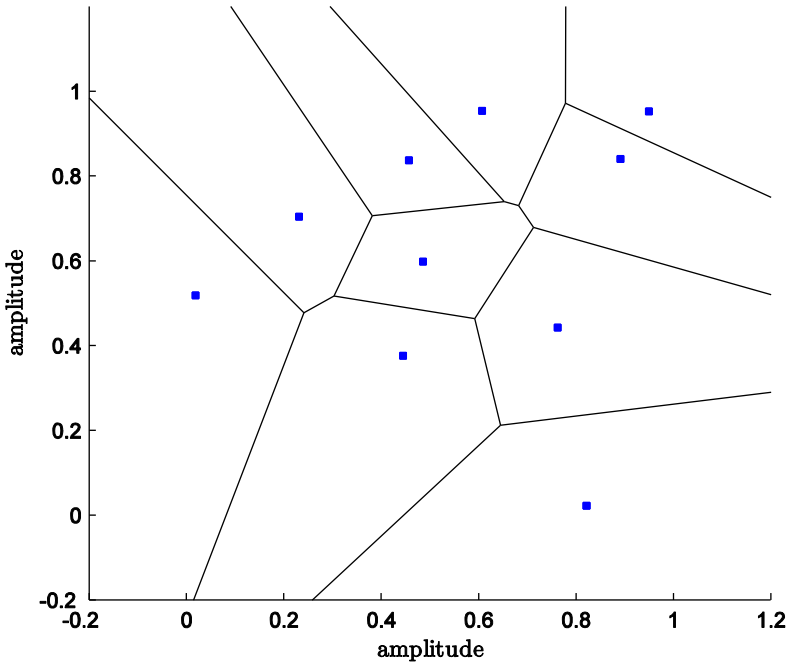

Figure 7.2 Decision boundaries for centroids based on Minimum Euclidean Distance

A two-dimensional decision region distribution based on minimum Minkowski distance with $p = 2$ is illustrated in Figure 7.2. Our target in this chapter is not to find a high-performance classifier, but rather to use a simple classifier to show that the feature vectors of glottal flow pulses do convey speaker identity information that differs from speaker to speaker.

Selection of Distinct Feature Patterns for Identifier

After glottal flow pulses have been estimated using the jointly parametric and nonparametric approach discussed in chapter 5, then speakers' parameterization results achieved by nonlinear least-square fitting of their estimated pulses based on minimization of ℓ^2 error can be considered feature vectors for a small scale text dependent identification system. Fixing the location - T_e of the maximum negative value E_e of the glottal pulses shown in Figure 7.3(a) and (c), we can align LF-fitted pulses from voiced utterances for all subjects to the same T_e. Then all fitted pulses are normalized by their values of E_e to scale all fitted pulses into the same measurable system. Then four scalars T_o, t_p, α and β are measured for both training data and testing data for each subject after LF-fitting using nonlinear least-square optimization. These scalars as results of parameterizations for those estimated pulses are fused into one feature vector which is fed into the identifier in Figure 7.1.

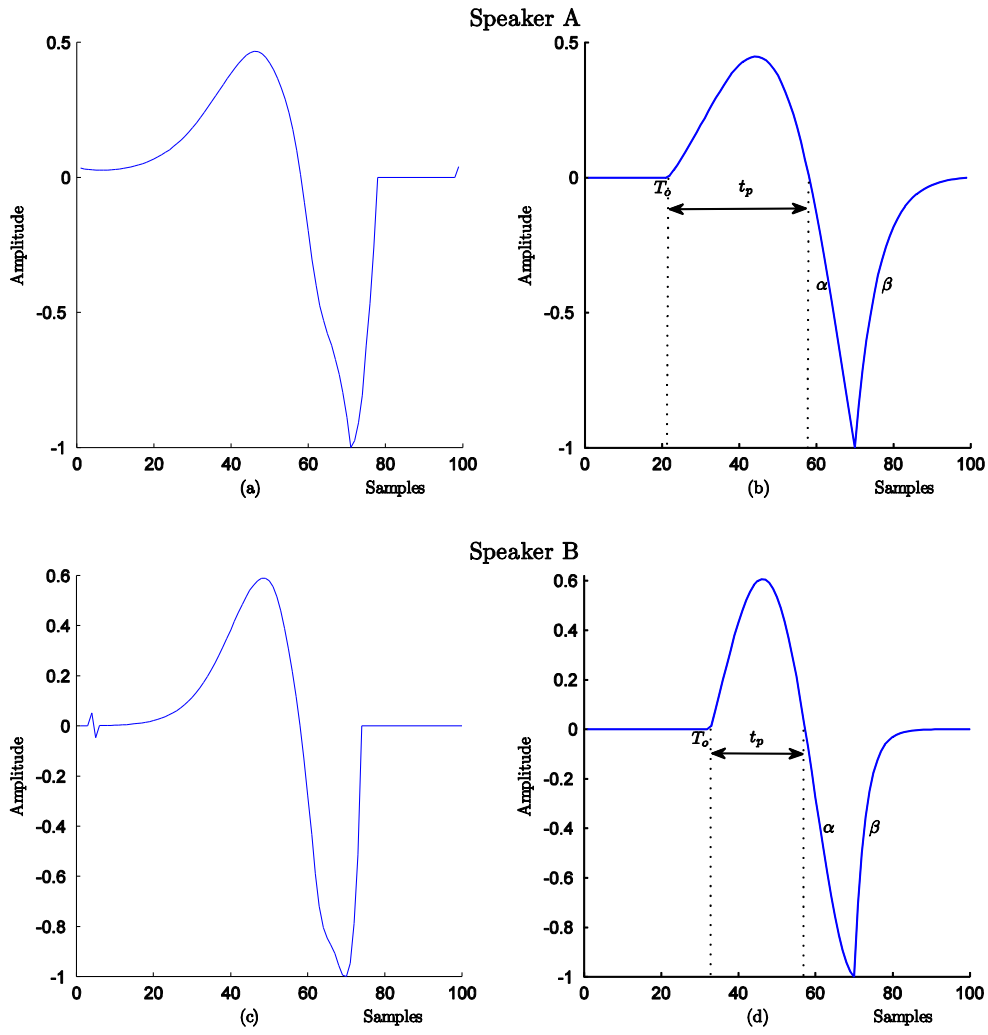

Figure 7.3 Illustrations of a single estimated glottal flow derivatives and their fitting pulses. (a) Estimated pulse for Speaker A (b) LF-fitting pulse with estimate parameters: $\boldsymbol{T_o = 21.67}$, $\boldsymbol{t_p = 36.4}$, $\boldsymbol{\alpha = 0.0345}$, $\boldsymbol{\beta = 0.167}$ (c) Estimated pulse for Speaker B (d) LF-fitting pulse with estimate parameters:$\boldsymbol{T_o = 32.79}$, $\boldsymbol{t_p = 24.5}$, $\boldsymbol{\alpha = 0.0206}$, $\boldsymbol{\beta = 0.346}$

The difference vector $\mathcal{D}_{\mathbf{x},\mathbf{y}_i}$between a testing feature pattern **x** and each training centroid $\mathbf{y}_i$ can be easily obtained by $\mathcal{D}_{\mathbf{x},\mathbf{y}_i} = |\mathbf{x} - \mathbf{y}_i|$ where an element $\mathcal{D}_{\mathbf{x},\mathbf{y}_i}(m) = \left|\mathbf{x}^{(m)} - \mathrm{y}_i^{(m)}\right|$. A deviation ratio vector $\boldsymbol{\rho}_i$ between the current testing vector **x** and all centroids **y** will be scaled by applying the Kronecker product of between $\mathcal{D}_{\mathbf{x},\mathbf{y}_i}$ and $\bar{\mathbf{y}}_i$ which is vector of reciprocals of the elements of centroid $\mathbf{y}_i$. Furthermore, the class label ϑ will be decided based on the minimum ℓ^1norm on $\boldsymbol{\rho}_i = \mathcal{D}_{\mathbf{x},\mathbf{y}_i} \otimes \bar{\mathbf{y}}_i$ between the current testing pattern **x** and the kth centroid $\mathbf{y}_i$.

The parameters shown in Figure 7.3 come from the optimum coefficients of Trust-Region fitting with the LF model (3.3) based on estimated pulses for a real speech voiced phoneme for the limited speaker population involved in the experiment. These LF model parameters T_o, t_p, α and β or other ones used for the geometrical representation of a class of waveforms will increasingly reduce the distance among distinct patterns if the body of subjects is expanded. Meanwhile, the fitting task, which is in fact an approximation to the observed function or sequence, will automatically remove some valuable information that probably contained in the estimation of glottal flow pulses or derivatives. Therefore, these two weaknesses closely associated with fitting parameters as feature patterns of speakers will increase the challenge of performing discrimination when more subjects are included in the tests.

Some existing mature identification systems [100] – [106] employing cepstrum coefficients or a variety of frequency coefficients as speaker features have demonstrated good performance. If any method of estimating information about glottal pulses is

effective, it should be possible to use this information to improve the overall identification performance.

A brief summary of a speaker-identification system based on complex cepstrum performance is now given. A group of complex cepstrum quantities $\hat{c}_x(\tau)$ for each pulse within one-pitch interval, generated by the windowed all-pole LP analysis and corresponding inverse filtering with those estimated coefficients for the LP model, are used to investigate whether excitation information of a speaker is contained in the estimated representation of complex cepstrum. Because $\hat{c}_x(\tau) = \hat{c}_{max}(\tau) + \hat{c}_{min}(\tau)$ where $\hat{c}_{max}(\tau)$ and $\hat{c}_{min}(\tau)$ denote cepstrum quantities in terms of maximum-phase and minimum-phase components [23], we can apply linear liftering to split $\hat{c}_{max}(\tau)$ and $\hat{c}_{min}(\tau)$ as what we did in chapter 5.

Complex cepstrum quantities corresponding to maximum-phase components of the estimated pulse after LP analysis and inverse filtering are therefore collected as feature vectors for the current speaker. As cepstrum quantities related to maximum-phase components mainly comes from LF model excitation source [13], [19], the representations of these components, with negative index in cepstrum frequency domain, can be used to formulate features for all subjects involved in the identifier. To check whether the glottal flow pulses carry information which can be used to help identify distinct subjects, training and testing features coming from estimated pulses for each subject are applied to the identifier in Figure 7.1.

Additionally, the complex cepstrum coefficients for a single glottal flow pulse for each term of two distinct speakers and the extracted portion to form feature vectors for these two speakers are shown in Figure 7.4.

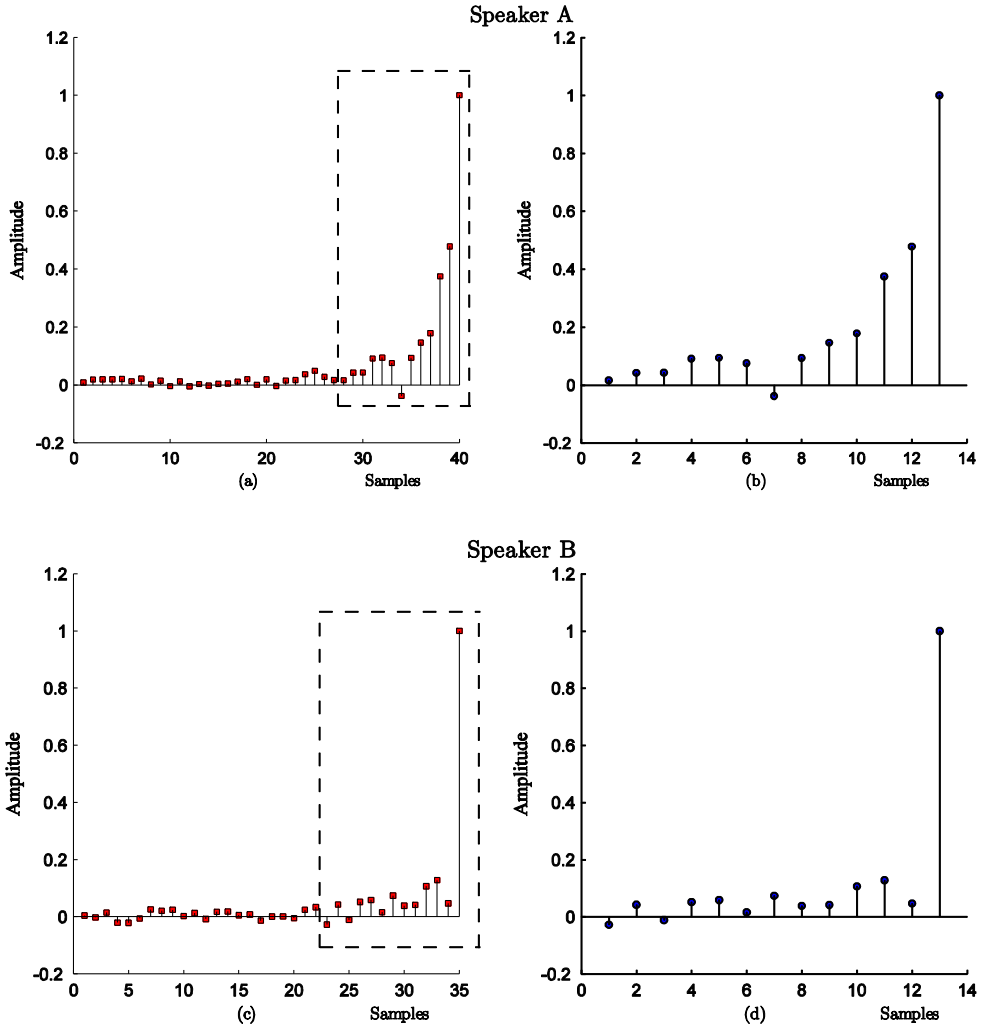

Figure 7.4 Illustrations of complex cepstrum coefficients of a single estimated glottal flow pulse and extraction of low cepstrum-frequency quantities. (a) complex cepstrum coefficients for Speaker A (b) quantities used for feature pattern about speaker A (c) complex cepstrum coefficients for Speaker B (d) quantities used for feature pattern about Speaker B

With glottal flow pulses estimated with the jointly parametric and nonparametric approach, 13 complex-cepstrum coefficient vectors $\hat{\mathbf{c}}_{max}$ corresponding to maximum-phase components for all speakers' were collected to form both training space $\mathcal{V}$ and testing space $\mathcal{U}$ as what we did when using LF fitting parameters. Difference vector $\mathcal{D}_{\mathbf{x},\mathbf{y}_i}$between a testing feature pattern $\mathbf{x}$ and each training centroid $\mathbf{y}_i$ can be obtained by $\mathcal{D}_{\mathbf{x},\mathbf{y}_i} = |\mathbf{x} - \mathbf{y}_i|_p$ as for LF model feature vectors. Furthermore, the class parameter ϑ will be decided based on the minimum Euclidean distance, $\left\|\mathcal{D}_{\mathbf{x},\mathbf{y}_i}\right\|_2$, between the current testing pattern $\mathbf{x}$ and the kth centroid $\mathbf{y}_i$. With 8 kHz sampled testing and training utterances of vowel /a/ from 12 distinct subjects, the identification performance for features from the LF-model and complex cepstrum coefficients corresponding to maximum-phase are summarized in Table 7.1.

Features	Correctness - %
LF-model parameters	83.3
CC parameters	75.0

Table 7.1 Speaker identification results for two different features

Inconsistent modes of phonation in terms of each subject: normal, pressed or breathy, could result in variations of estimated excitation waveforms even for the same speaker. This introduces variations and sensitivities to feature patterns used in the identifier. Thus, an identifier which employs only excitation information might be very inadequate without other speech information, especially with a large number of subjects.

However, combining features from the LF model with other speech features such as pitch or vocal-tract response will be expected to enhance speaker recognition system based on only one of these two feature sets.

CHAPTER EIGHT

CONCLUSIONS

This dissertation has investigated human speech production, source-tract interaction mechanisms and a variety of proposed glottal models that are central to the problem of estimating the periodic glottal excitation for voiced sounds or vowels. Although there exist some estimation schemes and some progress in the area of recovering the excitation information, they were restricted by some negative factors like strict assumptions and high computational complexities. Based on concerns about these limitations, we proposed two jointly parametric and nonparametric excitation estimation approaches, which employ phase decomposition without any assumed model type and just one step of LP analysis and inverse filtering for each flexible sliding window, to improve estimation results by using LP inverse filtering and homomorphic processing. Estimated glottal pulse parameters were evaluated for their effectiveness for a speaker identification using LF fitting model parameters and complex cepstrum coefficients as features. These features are used to estimate a speaker's glottal characteristics as voiced phonemes are pronounced.

Jointly Parametric and Nonparametric Excitation Estimation For Real and Synthetic Speech

Recovering the excitation signal of a voiced speech utterance is in fact an inverse problem where the source cannot be observed directly. This fact adds complexities to the evaluation of estimation results. The speech signal results from interactions of glottal

excitation, vocal-tract response and lips radiation. Linear system theory provides a theoretical basis for estimating the glottal excitations as is proposed in this dissertation. Different aspects of glottal excitation and vocal tract together with their combinational effects have been employed, including least-squares inverse filtering, IAIF, ZZT and CC. Each approach has its own advantages and restrictions. Our ultimate research goal was to discover new strategies to employ their advantages and minimize their weaknesses in a way to extract the glottal source information from speech utterances for voiced phonemes and to suppress the response of vocal tract in the process of recovering glottal source waveforms. Linear prediction and phase separation as two mature tools in speech analysis were combined to produce an enhancement to generate a smooth glottal pulse curve as shown in chapter 5. With the efficient use of frame-by-frame, odd-order LP analysis and its corresponding inverse filtering, the response of excitations from a speaker can be recovered. Multiple inverse filtering sections in IAIF [4] are no longer necessary in the process of recovering excitation information. Also, the accurate detection of glottal closure instants to fix two ending points of the analysis region for the following phase separation section to split maximum-phase components from minimum-phase components is also no longer necessary. Additionally, our method of frame-by-frame LP analysis and inverse filtering saves computation costs without precise detection of glottal closure instants and largely increases the robustness of the detection of these points in phase-separation.

Another approach employing third-order cummulants and the bicepstrum to refine the glottal waveform estimated from the previous LP analysis and inverse filtering was

thoroughly described in chapter 6. The third-order cumulants and the bicepstrum can largely reject the distortions because of mismatch in the process of cancelling vocal-tract effects due to inverse filtering. The estimated pulses were smooth and free of noises after the LP inverse filtering.

Two different evaluation schemes were used to evaluate the validity of the estimated pulses. Firstly, these two jointly parametric and nonparametric approaches were applied to a real vowel utterance from human speech and the results of estimating the glottal pulse were presented. Secondly, two synthetic pulses produced by different generation methods (1) convolution of two exponential sequences [39] and (2) using the LF model, are used to synthesize pulse trains to excite an artificial vocal-tract model represented by complex pole pairs, to generate a synthetic voiced speech utterance. The glottal pulse estimation method was applied to the synthetic utterance generated by the first method was directly compared with the synthetic pulse. And the estimation based on the utterance generated by the second method was be nonlinearly fitted by an LF model whose shape can be adjusted by several parameters [9]. These fitted parameters were further compared with those parameters used to synthesize LF-modeling pulses originally. Then the performance of the jointly parametric and nonparametric approaches was evaluated in terms of distinct types of synthetic excitation pulses as described above.

Features from Estimated Glottal Pulses for Speaker Identifier

The LF-fitted parameterization of estimated pulses for a speaker provides a feature vector as excitation information for him. The complex cepstrum quantities

corresponding to maximum-phase components were also clustered as feature vectors for different speakers. For either type of feature vectors, a small scale text-dependent speaker identification system was implemented. This system was based on the minimum-distance decision between the observed feature and centroids for all speakers. Although the population involved was small, the speaker identification experiments showed that glottal excitation parameters estimated by the proposed method performed better than complex cepstrum parameters obtained from the same data.

Suggested Directions of Research

The field of extraction of glottal source information is young and full of challenges. All speech processing domains that potentially employ bioinformatics could benefit from the addition of this type of information.

The problem of separating glottal source from vocal-tract information still presents challenges. The solution to this inverse problem will largely depend on new experimental and theoretical discoveries about interaction between source and vocal-tract components. With the help of these physical and theoretical explorations, better understanding of the roles played by both glottal pulses and vocal tract in the generation of voiced utterances will help researchers apply this knowledge to a variety of speech processing applications. Features which are byproducts of pulse estimation, along with maximum-phase cepstrum coefficients and other features from speakers, may be applied to speaker indentification with larger populations. The development of a robust speaker

identification system that can perform well in a degraded environment, like in telephone speech, should also benefit from the methods proposed in this dissertation.

APPENDICES

Appendix A

Third-Order Cumulant and Bicepstrum of Output from a Linear System Excited by White Processes

Let $X(n)$ be a 3rd order stationary process as the output of a linear system $h(n)$ excited by white noise $w(n)$, such that $X(n) = (w * h)(n) = \sum_k w(n-k)h(k)$. Then

1. $R_X^{(3)}(\tau_1, \tau_2) = \gamma_w^{(3)} \sum_k h(k)h(k+\tau_1)h(k+\tau_2)$
2. $\mathcal{C}_X^{(3)}(\omega_1, \omega_2) = \gamma_w^{(3)} H(\omega_1)H(\omega_2)H^*(\omega_1+\omega_2)$

Proof:

$$
\begin{aligned}
& R_X^{(3)}(\tau_1, \tau_2) \\
&= \mathbb{E}[X(n)X(n+\tau_1)X(n+\tau_2)] \\
&= \sum_{k_1,k_2,k_3} R_w^{(3)}(n-k_1, n+\tau_1-k_2, n+\tau_2-k_3)h(k_1)h(k_2)h(k_3) \\
&= \sum_{k_1,k_2,k_3} R_w^{(3)}(k_3-k_1-\tau_2, \tau_1-\tau_2-k_2+k_3)h(k_1)h(k_2)h(k_3) \\
&= \gamma_w^{(3)} \sum_{k_1,k_2,k_3} \delta(k_3-k_1-\tau_2)\delta(\tau_1-\tau_2-k_2 \\
&\qquad + k_3)h(k_1)h(k_2)h(k_3) \\
&= \gamma_w^{(3)} \sum_{k_3} h(k_3)h(k_3-\tau_2)h(\tau_1-\tau_2+k_3)
\end{aligned}
$$

Let $k = k_3 - \tau_2$, then

$$
\begin{aligned}
& \mathbb{E}[X(n)X(n+\tau_1)X(n+\tau_2)] \\
&= \gamma_w^{(3)} \sum_k h(k)h(k+\tau_1)h(k+\tau_2)
\end{aligned}
$$

Here, the proof of the 1st part is completed.Now we express the bispectrum $\mathcal{C}_X^{(3)}(\omega_1, \omega_2)$ in terms of $\mathrm{c}_X^{(3)}(\tau_1, \tau_2)$. Let $R_w^{(3)}(k_3 - k_1 - \tau_2, \tau_1 - \tau_2 - k_2 + k_3) = R_w^{(3)}(\mu + k_3 - k_1, \nu + k_3 - k_2)$ by setting $\mu = -\tau_2$ and $\nu = \tau_1 - \tau_2$. Then

$$\mathrm{c}_X^{(3)}(\tau_1, \tau_2) = \mathrm{c}_X^{(3)}(\mu, \nu) = \sum_{k_1,k_2,k_3} R_w^{(3)}(\mu + k_3 - k_1, \nu + k_3 - k_2) h(k_1) h(k_2) h(k_3)$$

So

$$\mathcal{C}_X^{(3)}(\omega_1, \omega_2) = \sum_{\mu,\nu} \sum_{k_1,k_2,k_3} \mathrm{c}_X^{(3)}(\mu, \nu) e^{-j(\omega_1 \mu + \omega_2 \nu)}$$

after arrangements,

$$\mathcal{C}_X^{(3)}(\omega_1, \omega_2) = \sum_{k_1,k_2,k_3} h(k_1) h(k_2) h(k_3) \left(\sum_{\mu,\nu} R_w^{(3)}(\mu + k_3 - k_1, \right.$$

$$\left. \nu + k_3 - k_2) e^{-j(\omega_1 \mu + \omega_2 \nu)} \right)$$

Substitute

$$\sum_{\mu,\nu} R_w^{(3)}(\mu + k_3 - k_1, \nu + k_3 - k_2) e^{-j(\omega_1 \mu + \omega_2 \nu)} = S_w(\omega_1, \omega_2) e^{j\omega_1(k_3 - k_1) + j\omega_2(k_3 - k_2)}$$

into $\mathcal{C}_X^{(3)}(\omega_1, \omega_2)$, we get

$$\mathcal{C}_w(\omega_1, \omega_2) = \sum_{k_1,k_2,k_3} h(k_1) h(k_2) h(k_3) S_w(\omega_1, \omega_2)\, e^{j\omega_1(k_3 - k_1) + j\omega_2(k_3 - k_2)}$$

Since $\mathrm{S}_w(\omega_1, \omega_2) = \gamma_w^{(3)}$ for statistical independent process, the above expression becomes

$$\sum_{k_1,k_2,k_3} h(k_1) h(k_2) h(k_3)\, e^{-j\omega_1 k_1 - j\omega_2 k_2 + j(\omega_1 + \omega_2) k_3}$$

Thus $C_X^{(3)}(\omega_1, \omega_2) = \gamma_w^{(3)} H(\omega_1) H(\omega_2) H^*(\omega_1 + \omega_2)$. The proof is completed. ■

REFERENCES

[1] G. Fant. *Acoustic theory of speech production*. Mouton, The Hague, The Netherlands. 1960.

[2] R. Miller. Nature of the vocal cord wave. *Journal of the Acoustical Society of America*, 31: 667–677, 1959.

[3] M. Matausek and V. Batalov. A new approach to the determination of the glottal waveform. *IEEE Transactions on Acoustics, Speech and Signal Processing*, 28:616-622, Dec. 1980.

[4] P. Alku. Glottal wave analysis with pitch synchronous iterative adaptive inverse filtering. *Speech Communication*, 11(2):109–118, 1992.

[5] P. Alku. An automatic method to estimate the time-based parameters of the glottal pulseform. *Proceeding of IEEE International Conference on Acoustics, Speech, and Signal Processing*, 2:29-32, 1992.

[6] A. Rosenberg. Effect of glottal pulse shape on the quality of natural vowels. *Journal of the Acoustical Society of America*, 49(2B):583–590, 1971.

[7] J. Deller, J. Hansen and J. Proakis. *Discrete-time processing of speech signals*, New York, Wiley-IEEE Press. 1999.

[8] T. Raitio, A. Suni, J. Yamagishi, H. Pulakka, J. Nurminen, M. Vainio and P. Alku. HMM-based speech synthesis utilizing glottal inverse filtering. *IEEE Transactions on Audio, Speech & Language Processing*, 19(1): 153-165, 2011

[9] D. Klatt and L. Klatt. Analysis, synthesis, and perception of voice quality variations among female and male talkers. *Journal of the Acoustical Society of America*, 87(2):820–857, 1990.

[10] G. Fant, J. Liljencrants, and Q.-G. Lin. A four-parameter model of glottal flow. *STL-QPSR*, 26(4):1–13, 1985.

[11] M. Plumpe, T. Quatieri and D. Reynolds. Modeling of the glottal flow derivative waveform with application to speaker identification. *IEEE Transactions on Speech and Audio Processing*, 7(5):569–586, Sep. 1999.

[12] G. Fant. The LF-model revisited. Transformations and frequency domain analysis. *STL-QPSR*, 36(2-3):119–156, 1995.

[13] B. Doval, C. d'Alessandro, and N. Henrich. The voice source as a causal/anticausal linear filter. *Proceeding of ISCA Voice Quality: Functions, Analysis and Synthesis (VOQUAL)*, 16–20, 2003.

[14] J. Flanagan. Note on the design of "terminal-analog" speech synthesizers. *Journal of the Acoustical Society of America*, 29:306–310, 1957b.

[15] J. Flanagan. Some properties of the glottal sound source. *Journal of Speech and Hearing Research*, 1:99–116, 1958.

[16] W. Mason. The approximate networks of acoustic filters. *Journal of the Acoustical Society of America*, 1(2A): 263-272, 1930.

[17] I. Lim and B. Lee. Lossless pole-zero modeling of speech signals. *IEEE Transactions on Speech and Audio Processing*, 1(3):269–276, Jul. 1993.

[18] L. Rabiner and R. Schafer. *Digital processing of speech signals*. Englewood Cliffs, Prentice Hall, 1978.

[19] B. Bozkurt, B. Doval, C. D'Alessandro and T. Dutoit. Zeros of Z-transform representation with application to source-filter separation in speech. *IEEE Signal Processing Letters*, 12(4):344–347, Apr. 2005.

[20] J. Deller. On the time domain properties of the two-pole model of the glottal waveform and implications for LPC. *Speech Communication: An Interdisciplinary Journal*, 2:57–63, 1983.

[21] D. Y. Wang, J. D. Markel and A.H. Gray. Least squares glottal inverse filtering from the acoustic speech waveform. *IEEE Transactions on Acoustics, Speech, And Signal Processing*, ASSP-27(4):350–355, Aug. 1979.

[22] K. Funaki, Y. Miyanaga and K. Tochinai. Recursive ARMAX speech analysis based on a glottal source model with phase compensation. *Signal Processing*, 74:279–295, 1999.

[23] A. Oppenheim. *Discrete-Time Signal Processing*. 3rd ed., Upper Saddle River, Prentice Hall. 2009.

[24] J. Demmel. *Applied Numerical Linear Algebra*, SIAM. Aug. 1997.

[25] D. Manolakis, V. Ingle and S. Kogon. *Statistical and adaptive signal processing: spectral estimation, signal modeling, adaptive filtering and array processing*. Artech House Signal Processing Library. 2005.

[26] J. Proakis, C. Rader, F. Lin, M. Moonen, I. Proudler, C. Nikias. *Algorithms for statistical signal processing*. Prentice Hall, 2002.

[27] A. Yeredor. The extended least squares criterion: minimization algorithms and application. *IEEE Transactions on Signal Processing.* 49(1):74–86, Jan. 2000.

[28] D. Feng, Z. Bao and L. Jiao. Total least mean squares algorithm. *IEEE Transactions on Signal Processing*. 46(8):2122–2130, Aug. 1998.

[29] S. Chandra and L. Wen. Experimental comparison between stationary and nonstationary formulations of linear prediction applied to voiced speech analysis. *IEEE Transactions on Signal Processing*. 22(6):403–415, 1974.

[30] P. Murthy and B. Yegananarayana. Robustness of group-delay-based method for extraction of significant instants of excitation from speech signals, *IEEE Transactions on Speech and Audio Processing*. 7(6):609–619, Nov. 1999.

[31] P. Naylor, A. Kounoudes, J. Gudnason, and M. Brookes. Estimation of glottal closure instants in voiced speech using the DYPSA algorithm. *IEEE Transactions on Speech Audio Processing*. 15(1):34–43, Jan. 2007.

[32] R. Smits and B. Yegnanarayana. Determination of instants of significant excitation in speech using group delay function. *IEEE Transactions on Speech and Audio Processing*. 3(5):325-333, Sep. 1995.

[33] M. Thomas and P. Naylor. The sigma algorithm: A glottal activity detector for electroglottographic signals. *IEEE Transactions on Audio, Speech, and Lang. Processing*. 17(8):1557–1566, Nov. 2009.

[34] E. Abberton, D. Howard, and A. Fourcin. Laryngographic assessment of normal voice: A tutorial. *Clinical Linguist. Phon.*, 3:281–296, 1989.

[35] T. Drugman, B. Bozkurt and T. Dutoit. Complex cepstrum-based decomposition of speech for glottal source estimation. *Proceedings of Interspeech*, 2009.

[36] J. Makhoul. Linear prediction: A tutorial review. *Proceedings of the IEEE*, 63:561–580, Apr. 1975.

[37] T. Tremain. The government standard linear predictive coding algorithm: LPC-10. *Speech Technology*, 1:40–49, Apr. 1982.

[38] T. Drugman, B. Bozkurt and T. Dutoit. Causal–anticausal decomposition of speech using complex cepstrum for glottal source estimation. *Speech Communication*. 53(6):740–741, Jul. 2011.

[39] T. Quatieri. *Discrete-Time Speech Signal Processing*. Upper Saddle River, Prentice Hall. 2001.

[40] R. Schaback. Convergence analysis of the general Gauss-Newton method. *Numerische Mathematik*, 46:281-309, 1985.

[41] L. Lasdon and A. Waren. Survey of Nonlinear Programming Applications. *Operations Research*. 28(5):1029–1073, 1980

[42] N. Jorge and J. Stephen. *Numerical Optimization*. 2nd ed., Springer. Jul. 2006

[43] C. Kelley. Iterative Methods for Optimization. *SIAM Frontiers in Applied Mathematics*, 18, 1999

[44] T. Strutz. Data Fitting and Uncertainty: *A practical introduction to weighted least squares and beyond*. Vieweg and Teubner. Nov. 2010

[45] S. Gratton. A. Lawless and N. Nichols. Approximate Gauss-Newton methods for nonlinear least squares problems. *SIAM Journal on Optimization*, 18(1), Feb. 2007

[46] D. Bates and D. Watts. *Nonlinear Regression and Its Applications*. New York: Wiley, 1988.

[47] D. Gorinevsky. An approach to parametric nonlinear least square optimization and application to task-level learning control. *IEEE Transactions on Automatic Control*, 42(7):912–927, Jul. 1997

[48] J. Dennis, D. Gay and R. Welsch. An adaptive nonlinear least-squares algorithm. *ACM Transactions on Mathematical Software*, 7:348–368, Sept. 1981.

[49] K. Levenberg. A method for the solution of certain problems in least squares. *Quarterly of Applied Mathematics*, 2:164–168, 1944.

[50] D. Marquardt. An Algorithm for Least-Squares Estimation of nonlinear parameters. *Journal of the Society for Industrial and Applied Mathematics*, 11(2):431–441, 1963

[51] X. Luo, L. Liao and H. Tam. Convergence analysis of the Levenberg-Marquardt method. *Optimization Methods and Software*, 22(4):659–678, Aug. 2007

[52] J. Dennis and L. Vincente. Trust-region interior-point algorithms for minimization problems with simple bounds. *SIAM Journal of Control and Optimization*, TR94–42, Nov, 1994

[53] T. Coleman and Y. Li. An interior trust region approach for nonlinear minimization subject to bounds. *SIAM Journal on Optimization*, 6(2):418–445, 1996

[54] J. Dennis, M. Heinkenschloss and L. Vincente. Trust-Region Interior-Point SQP Algorithms for a Class of Nonlinear Programming Problems. *SIAM Journal of Control and Optimization*, 36(5):1750–1794, 1998

[55] R. Byrd, J. Gilbert and J. Nocedal. A Trust Region Method Based on Interior Point Techniques for Nonlinear Programming. *Mathematical Programming*, 89(1):149–185, 2000.

[56] J. More. *Recent developments in algorithms and software for trust-region methods*. In A. R. Bachem, M. Grotshel and B. Korte, Eds., Mathematical Programming: The State of the Art, Springer-Verlag, Berlin, 258–287, 1983.

[57] Y. Yuan. On the convergence of trust region algorithm. *Mathematica Numerica Sinica*, 16(3):333–346, 1996.

[58] A. Conn, N. I. Gould and P. Toint. *Trust region methods*. Philadelphia, MPS-SIAM Series on Optimization, SIAM, 2000.

[59] F. Bastin, V. Malmedy, M. Mouffe, P. Toint and D. Tomanos. A retrospective trust-region method for unconstrained optimization. *Mathematical Programming*, 123(2): 395–418, 2010.

[60] X. Zhang, Z. Chen and J. Zhang. A self-adaptive trust region method unconstrained Optimization. *Operations Research Transactions*, 5(1):53–62, 2001.

[61] N. Karmarkar. A new polynomial time algorithm for linear programming. *Combinatorica*, 4(4):373–395, 1984.

[62] S. Mehrotra. On the implementation of a primal-dual interior point method. *SIAM Journal on Optimization*, 2(4): 575–601, 1992.

[63] F. Potra and S. Wright. Interior-point methods. *Journal of Computational and Applied Mathematics*, 124:281–302, 2000.

[64] A. Forsgren, P. Gill and M. Wright. Interior methods for nonlinear optimization. *SIAM* Rev.44, 525–597, 2002.

[65] F. Potra. Q-superlinear convergence of the iterates in primal-dual interior-point methods. *Math. Programming*, 91(Ser.A):99–115, 2001.

[66] C. Kelley, *Solving nonlinear equations with Newton's method*. SIAM. 2003.

[67] W. Press, B. Flannery, S. Teukolsky and W. Vetterling. "*General Curve Fit"*, Numerical Recipes in C. Cambridge University Press. 1988.

[68] W. Press, B. Flannery, S. Teukolsky and W. Vetterling. "*Cubic Spline Curve Fit"*, Numerical Recipes in C. Cambridge University Press. 1988.

[69] J. Wolberg. Data analysis using the method of least squares: *Extracting the most information from experiments*. 1st ed., Springer, Feb. 2006.

[70] S. Ahn. *Least squares orthogonal distance fitting of curves and surfaces in space*. 1st ed., Springer. Jan. 2005.

[71] H. Wang, Y. Ge, Z. Liu; H. Liu, L. Xu. One curve-fit method for the evaluation of the total distortion of sinusoidal signal. *Proceedings of IEEE International Conference on Information and Automation (ICIA),* 2010.

[72] P. Scott. Minimax and L_1 curve fitting in non-Gaussian MAP estimation. *IEEE Transactions on Automatic Control*, 20(5):690–691, 1975.

[73] N. Greggio, A. Bernardino, C. Laschi, P. Dario and J. Santos-Victor. An Algorithm for the Least Square-Fitting of Ellipses. *Proceedings of IEEE International Conference on Tools with Artificial Intelligence (ICTAI)*, 351–353, 2010.

[74] A. Papoulis and S. Pillai. *Probability, random variables and stochastic processes*. 4th ed., McGraw-Hill. 2002.

[75] W. Collis, P. White and J. Hammond. High-order spectra: the bespectrum and trispectrum. *Mechanical Systems and Signal Processing*, 12(3):375–394, May 1998.

[76] T. Hall and G. Giannakis. Bispectral Analysis and Model validation of Texture Images. *IEEE Transactions on Image Processing*, 4(7):996–1009, Jul. 1995.

[77] Y. Wu and A. Leyman. Time delay estimation in unknown spatially correlated Gaussion noises using higher-order statistics, *Proceedings of IEEE International Conference on Acoustics, Speech and Signal Processing*, 2813–2816, 1999.

[78] D. Ruiz and A. Gallego. Bispectrum estimation using AR-modelling. *The International Journal for Computation and Mathematics in Electrical and Electronic Engineering*, 18(1):43–60, 1999.

[79] A. Petropulu, and C. Nikias. The complex cepstrum and bicepstrum: analytic performance evaluation in the presence of Gaussian noise. *IEEE Transactions on Acoustics, Speech and Signal Processing*, 38(7):1246–1256, Jul. 1990.

[80] P. Molchanov, J. Astola, K. Egiazarian and A. Totsky. Moving target classification in ground surveillance radar ATR system by using novel bicepstral-based information features. *European Radar Conference (EuRAD)*, 194–197, 2011.

[81] Y. Zhou, Y. Liu, H. An and L. Che. Higher order spectral analysis for vibration signals of the large steam turbine in slow-down process. *Proceedings of IEEE International Conference on Intelligent Control and Information Processing (ICICIP)*, 1149–1154, 2011.

[82] H. Hsieh, H. Chang and M. Ku. Higher-order statistics based sequential spectrum sensing for cognitive radio. *Proceedings of IEEE International Conference on ITS Telecommunications (ITST)*, 696–701, Aug. 2011.

[83] P. Shih and D. Chang. An automatic modulation classification technique using high-order statistics for multipath fading channels. *Proceedings of IEEE International Conference on ITS Telecommunications (ITST)*, 691–695, Aug. 2011.

[84] C. Nikias and J. Mendel. Signal Processing with Higher-Order Spectra. *IEEE Signal Processing Magazine*, 10:10–37, Jul. 1993.

[85] E. Nemer, R. Goubran and S. Mahmoud. Robust voice activity detection using higher-order statistics in the LPC residual domain. *IEEE Transactions on Speech and Audio Processing*, 9(3):217–231, Mar. 2001.

[86] R. Pan and C. Nikias. The complex cepstrum of higher order cumulants and nonminimum phase system identification. *IEEE Transactions on Acoustics, Speech and Signal Processing*, 36(2):186–205, Feb. 1988.

[87] A. Petropulu and U. Abeyratne. System reconstruction from higher order spectra slices. *IEEE Transactions on Signal Processing*, 45(9):2241–2251, Sept. 1997.

[88] D. Newland. *An Introduction to Random Vibrations, Spectral & Wavelet Analysis*. 3rd ed., Dover Publications, Jul. 2005.

[89] J. Mendel. Tutorial on higher-order statistics (spectra) in signal processing and system theory: theoretical results and some applications. *Proceedings of the IEEE*, 79(3):278–305, Mar. 1991.

[90] J. Campbell. Speaker recognition: a tutorial. *Proceedings of the IEEE*, 85(9):1437–1462, Mar. 1997.

[91] D. Reynolds. *A Gaussian mixture modeling approach to text-independent speaker identification*. Ph.D. Thesis, Georgia Institute of Technology, Sept. 1992.

[92] H. Gish and M. Schmidt. Text-independent speaker identification. *IEEE Signal Processing Magazine*, 11(4):18–32, 1994.

[93] R. Gray. Vector Quantization. *IEEE Transactions on Acoustics, Speech and Signal Processing*, 1(2):4–29, Apr. 1984.

[94] C. Yen, C. Young and M. Nagurka. A vector quantization method for nearest neighbor classifier design. Pattern Recognition Letters, 25(6): 725–731, Apr. 2004.

[95] B. Dasarathy. *Nearest neighbor: pattern classification techniques*. Hoboken, IEEE Press, 1990.

[96] P. Fränti, O. Virmajoki and V. Hautamäki. Fast agglomerative clustering using a k-nearest neighbor graph. *IEEE Trans. on Pattern Analysis and Machine Intelligence*, 28 (11):1875-1881, Nov. 2006.

[97] S. Dasgupta and Y. Freund. Random projection trees for vector quantization. *IEEE Transactions on Information Theory*, 55(7): 3229–3242, Jul. 2009.

[98] P. Nguyen, M. Akagi, T. Ho. Temporal decomposition: a promising approach to VQ-based speaker identification. *Proceedings of IEEE International Conference on Acoustics, Speech and Signal Processing (ICASSP)*, I184–I187, 2003.

[99] S. Garcia, J. Derrac, J. Cano and F. Herrera. Prototype selection for nearest neighbor classification: taxonomy and empirical study. *IEEE Transactions on Pattern Analysis and Machine Intelligence*, 34(3): 417–435, Mar. 2012.

[100] A. Jain, N. Prakash and S. Agrawal. Evaluation of MFCC for emotion identification in Hindi speech. *Proceedings of IEEE International Conference on Communication Software and Networks (ICCSN)*, 189–193, 2011.

[101] A. Revathi and Y. Venkataramani. Text independent composite speaker identification/verification using multiple features. *Proceedings of IEEE World Congress on Computer Science and Information Engineering*, 257–261, 2009.

[102] Y. Shao and D. Wang. Robust speaker recognition using binary time-frequency masks. *Proceedings of IEEE International Conference on Acoustics, Speech and Signal Processing (ICASSP)*, 1520–6149, 2006.

[103] J. Gudnason and M. Brookes. Voice source cepstrum coefficients for speaker identification. *Proceedings of IEEE International Conference on Acoustics, Speech and Signal Processing (ICASSP)*, 4821–4824, 2008.

[104] S. Biswas, S. Ahmad and M. Islam Mollat. Speaker identification using cepstral based features and discrete hidden markov model. *Proceedings of IEEE International Conference on Information and Communication Technology (ICICT)*, 303–306, 2007.

[105] F. Castaldo, E. Dalmasso, P. Laface, D. Colibro and C. Vair. Language identification using acoustic models and speaker compensated cepstral-time matrices. *Proceedings of IEEE International Conference on Acoustics, Speech and Signal Processing (ICASSP)*, IV1013–IV1016, 2007.

[106] F. Xing and J. Hansen. Speaker identification within whispered speech audio streams. *IEEE Transactions on Audio, Speech, and Language Processing*, 19(5):1408–1421, Jul. 2011.